arXiv:hep-ph/9707326v1 11 Jul 1997

CERN-TH/97–158

NON-FACTORIZABLE CORRECTIONS TO W-PAIR PRODUCTION: METHODS AND ANALYTIC RESULTS

W. Beenakker$^{*)}$, **A.P. Chapovsky**$^{\dagger)}$

Instituut–Lorentz, University of Leiden, The Netherlands

and

F.A. Berends

Theory Division, CERN, CH–1211 Geneva 23, Switzerland

and

Instituut–Lorentz, University of Leiden, The Netherlands

ABSTRACT

In this paper we present two methods to evaluate non-factorizable corrections to pair-production of unstable particles. The methods are illustrated in detail for W-pair-mediated four-fermion production. The results are valid a few widths above threshold, but not at threshold. One method uses the decomposition of n-point scalar functions for virtual and real photons, and can therefore be generalized to more complicated final states than four fermions. The other technique is an elaboration on a method known from the literature and serves as a useful check. Applications to other processes than W-pair production are briefly mentioned.

CERN-TH/97–158
July 1997

$^{*)}$Research supported by a fellowship of the Royal Dutch Academy of Arts and Sciences.
$^{\dagger)}$Research supported by the Stichting FOM.

1 Introduction

With the start of LEP2, quantitative knowledge of the radiative corrections to the four-fermion production process $e^+e^- \to 4f$ is needed [1]. The full calculation of all these corrections will be extremely involved and at present one relies on approximations [1], such as leading-log initial-state radiation and running couplings [2]. Another approach is to exploit the fact that the corrections, in particular those associated with the production of an intermediate W-boson pair, are important. This (charged-current) production mechanism dominates at LEP2 energies and determines the LEP2 sensitivity to the mass of the W boson and to the non-Abelian triple gauge-boson interactions. As such, one could approximate the complete set of radiative corrections by considering only the leading terms in an expansion around the W poles. The double-pole residues thus obtained could be viewed as a gauge-invariant definition of corrections to "W-pair production". The sub-leading terms in this expansion are generically suppressed by powers of Γ_W/M_W, with M_W and Γ_W denoting the mass and width of the W boson. The quality of this double-pole approximation degrades in the vicinity of the W-pair production threshold, but a few Γ_W above threshold it is already quite reliable [3]. It is conceivable that in the near future a combination of the above-mentioned approximations will result in sufficiently accurate theoretical predictions for four-fermion production processes.

In the double-pole approximation the complete set of first-order radiative corrections to the charged-current four-fermion processes can be divided into so-called factorizable and non-factorizable corrections [1, 3], i.e. corrections that manifestly contain two resonant W propagators as overall factors and those that do not. In view of gauge-invariance requirements, some care has to be taken with the precise definition of this split-up (see below). In the factorizable corrections one can distinguish between corrections to W-pair production and W decay. In this paper we give a detailed account of the non-factorizable corrections that were used in the analysis of [4]. From the complete set of electroweak Feynman diagrams that contribute to the full $\mathcal{O}(\alpha)$ correction, we will therefore only consider the non-factorizable ones, both for virtual corrections and real-photon bremsstrahlung. To be more precise, since we are only interested in the double-pole terms we are led to consider only non-factorizable QED diagrams in the soft-photon limit. This means that we use simplified expressions for loop corrections and real-bremsstrahlung interferences, i.e. the photon momentum k^μ is neglected in the numerators and whenever possible k^2 is neglected in the denominators. It does not mean that the photon energy is taken to be small in the actual loop/phase-space integrations. In fact, for real bremsstrahlung the photon is treated inclusively and the energy is extended to infinity, which simplifies and approximates the phase-space integrals [5]. The errors associated with this procedure are formally of higher order in the expansion in powers of Γ_W/M_W in the energy region where $\Delta E \approx M_W$, since photons with an energy of $\mathcal{O}(M_W)$ force the W-bosons off the resonance [5]. Here ΔE stands for the distance in energy to the threshold. In the energy region where $\Gamma_W \ll \Delta E \ll M_W$, the accuracy of the approximation becomes of $\mathcal{O}(\Gamma_W/\Delta E)$. Finally, near threshold, where $\Delta E \approx \Gamma_W$, our approximation breaks down. There the dominant correction comes from the Coulomb effect, which was discussed in great detail in the literature (see e.g. [6, 7, 8]).

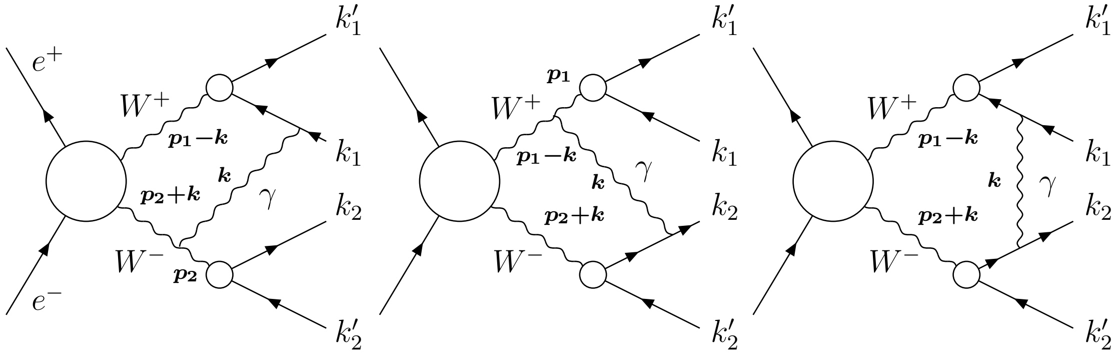

$\boldsymbol{D_{0123}}$ $\boldsymbol{D_{0124}}$ $\boldsymbol{E_{01234}}$

Figure 1: Virtual diagrams contributing to the manifestly non-factorizable W-pair corrections in the purely leptonic case. The scalar functions corresponding to these diagrams are denoted by D_{0123}, D_{0124}, and E_{01234}.

The above approach is the same as the one adopted by the authors of Ref. [9], who were the first to calculate non-factorizable W-pair corrections. For the present calculations, we have used two different methods. One is an extension of the treatment in [9], the other is a modification of the standard methods, which involves a combination of the decomposition of multipoint scalar functions and the Feynman-parameter technique. The results obtained with our two methods are in complete mutual agreement. However, in contrast to [9], a clear separation between virtual and real photonic corrections has been made in both methods, which is essential to establish the cancellations of infrared and collinear divergences. This treatment reveals a significant difference between our results and those obtained by the authors of [9]. Our final results do not contain any logarithmic terms involving the final-state fermion masses, whereas in the results of [9] explicit logarithms of fermion-mass ratios occur (see discussion in Sect. 4.1 of Ref. [9]). This difference can be traced back to the fact that although the fermion masses can formally be neglected in the absence of collinear divergences, they have to be introduced in intermediate results in order to regularize those divergences before dropping out from the final results.

1.1 Gauge-invariant definition of non-factorizable corrections

In order to give a gauge-invariant definition of the non-factorizable QED corrections in the soft limit, we first restrict ourselves to the manifestly non-factorizable corrections, i.e. those not having two resonant W-propagators as explicit overall factors. In addition we will restrict ourselves to the simplest class of charged-current four-fermion processes, involving a purely leptonic final state:

$$e^+(q_1)e^-(q_2) \to W^+(p_1) + W^-(p_2) \to \nu_\ell(k_1')\ell^+(k_1) + \ell'^-(k_2)\bar{\nu}_{\ell'}(k_2'). \tag{1}$$

Whenever possible, all external fermions are taken to be massless. The relevant contributions consist of the final–final and intermediate–final state photonic interactions displayed in Fig. 1.

In principle also manifestly non-factorizable vertex corrections exist, which arise when the photon in Fig. 1 does not originate from a W-boson line but from the $\gamma WW/ZWW$ vertex (hidden in the central blob). Those contributions can be shown to vanish in the double-pole approximation, using power-counting arguments [1]. Also the manifestly non-factorizable initial–final state interference effects disappear in our approach. This happens upon adding virtual and real corrections, as will be briefly explained later.

The double-pole contribution of the virtual corrections to the differential cross-section can be written in the form

$$d\sigma_{\mathrm{virt}} = 32\pi\alpha\, \mathrm{Re}\Big[i(p_2\cdot k_1)D_1 D_{0123} + i(p_1\cdot k_2)D_2 D_{0124} + i(k_1\cdot k_2)D_1 D_2 E_{01234}\Big]\, d\sigma_{\mathrm{Born}}, \qquad (2)$$

where $D_{1,2} = p_{1,2}^2 - M_W^2 + iM_W\Gamma_W$ are the inverse (Breit–Wigner) W-boson propagators. The functions D_{0123}, D_{0124}, and E_{01234} are the scalar integrals corresponding to the diagrams shown in Fig. 1, with the integration measure defined as $d^4k/(2\pi)^4$. The propagators occurring in these integrals are labelled according to: 0 = photon, $1 = W^+$, $2 = W^-$, $3 = \ell^+$, and $4 = \ell^-$. Note that the factorization property exhibited in Eq. (2) is a direct consequence of the soft-photon approximation, which is inherent in our approach. As a result, the propagators hidden inside the central blobs of Fig. 1 are Born-like, i.e. unaffected by the presence of the non-factorizable photonic interactions.

In a similar way, only interferences of the real-photon diagrams can give contributions to the manifestly non-factorizable corrections. The relevant interferences can be read off from Fig. 1 by taking the exchanged photon to be on-shell. The infrared divergences contained in the virtual corrections will cancel against those present in the corresponding bremsstrahlung interferences.

The set of manifestly non-factorizable QED diagrams displayed in Fig. 1 is not $U(1)$ gauge invariant, which can be explicitly seen from the non-vanishing of gauge-parameter-dependent terms when a general covariant gauge is used for the photon propagators. In order to achieve a gauge-invariant definition of the non-factorizable corrections, all (soft) photonic interactions between the positively (e^+, W^+, ℓ^+) and negatively (e^-, W^-, ℓ'^-) charged particles should be taken into account, which also holds for hadronic final states. Looking at Fig. 1, this is equivalent to the set of all up–down QED interferences. The gauge invariance of these interference effects is a direct consequence of the fact that in the soft-photon approximation the matrix element can be viewed as a product of two conserved currents: one, where the soft photon is attached to the positively charged particles, and one, where it is attached to the negatively charged ones. Only three of those up–down QED interferences are already present in Fig. 1, all others except one will vanish in the soft-photon approximation. In the soft-photon, double-pole approximation it is the "Coulomb" interaction between the off-shell W bosons that survives as an extra contribution to the differential cross-section (see Fig. 2):

$$d\sigma^{\mathrm{C}}_{\mathrm{virt}}(p_1|p_2) = 32\pi\alpha\, \mathrm{Re}\Big[i(p_1\cdot p_2)C_{012}\Big]\, d\sigma_{\mathrm{Born}}. \qquad (3)$$

The scalar three-point function C_{012} is defined according to the above-defined notation. The terminology "Coulomb" interaction should not lead to confusion. It is a contribution that is

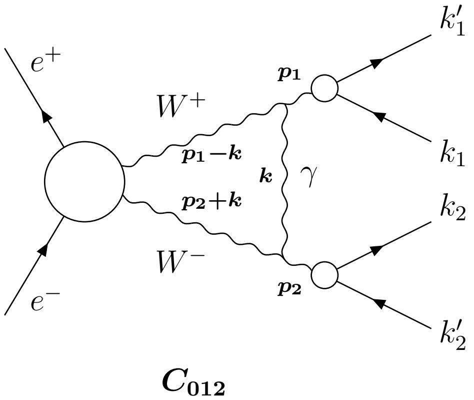

Figure 2: The gauge-restoring "Coulomb" contribution. The corresponding scalar function is denoted by C_{012}. In Sect. 3.3 we shall briefly indicate the distinction between our "Coulomb" contribution, valid outside the threshold region, and the usual one, which is also valid inside that region.

a part of the diagram in Fig. 2. In Sect. 3.3 we shall briefly indicate the distinction between our "Coulomb" contribution, valid outside the threshold region, and the usual one, which is primarily valid inside that region.

From the diagrams in Fig. 1 it is clear that we have to calculate four- and five-point scalar functions and related bremsstrahlung interference expressions, all in the soft-photon approximation. In the next two sections we focus on the analytical results as obtained with the modified standard technique (MST), consisting of various elements. In particular the decomposition of the virtual and real five-point functions into a sum of four-point functions is given some special attention in Sect. 2.[1] As such, the basic building blocks of the MST are the four-point functions D and the related bremsstrahlung interference terms D^{R}. A general relation between the two entities is discussed in Sect. 2.4. As a final step we derive in Sect. 3 the relevant scalar four-point functions D in the soft-photon approximation by applying the Feynman-parameter technique. The related D^{R} functions are obtained by using a "particle-pole" expression and performing certain substitutions.

In Sect. 4 we present the calculation along the lines of Ref. [9], which involves the method of direct momentum integration. This calculation will serve as a check of the MST results. Moreover, it is required for pinpointing the source of the differences with [9]. Whereas the method of Sects. 2 and 3 seems to be quite general, the method of Sect. 4 is unlikely to be applied to n-point functions with $n > 5$. As we will see, it just becomes too complicated.

In Sect. 5 we present the main analytical features of our study and we indicate how the results for semileptonic and hadronic final states can be obtained from the purely leptonic case. For the numerical implications of the non-factorizable corrections we refer to [4]. Our calculations confirm that non-factorizable corrections vanish in the special case of initial–final state interference, thereby making non-factorizable radiative corrections independent from the W production angle, and in all cases when the integrations over both invariant masses of the virtual W bosons are performed [5]. The practical consequence of the latter is that pure angular distributions are unaffected by non-factorizable $\mathcal{O}(\alpha)$ corrections. So, the studies of non-Abelian triple gauge-boson couplings at LEP2 [10] are not affected by these corrections. The non-factorizable $\mathcal{O}(\alpha)$ corrections, however, do affect the invariant-mass distributions (W line-shapes). These distributions play a crucial role in extracting the W-boson mass from the data through direct reconstruction of the Breit–Wigner resonances. The non-factorizable corrections to the line-shapes turn out to be the same for quark and lepton final states, provided the integrations over the decay angles have been performed. Finally, in Sect. 6 we draw some conclusions.

---

[1] For higher n-point functions ($n > 5$) this decomposition can be carried out in an analogous way. Thus in principle the methods outlined in Sects. 2.1 and 2.2 provide the basic tools for considering more involved non-factorizable corrections, e.g. for six-fermion final states.

2 Modified standard technique: basic ingredients

In this section the basic ingredients are presented for the evaluation of non-factorizable corrections in the MST. As a first step we discuss the decomposition of virtual and real five-point functions into a sum of four-point functions. Subsequently we demonstrate how virtual and real contributions can be related in the soft-photon approximation. Having established the five-point decompositions and the relation between virtual and real contributions, the actual calculation in the MST boils down to the evaluation of scalar four-point integrals.

2.1 Decomposition of the virtual five-point function

In this subsection we derive the decomposition of the virtual scalar five-point function into a sum of scalar four-point functions. The derivation follows Ref. [11]. The reason for repeating this calculation lies in the fact that it will serve as guideline for the decomposition of the real five-point function, which has not been considered before.

Let us consider the following general five-point function:

$$E_{01234} = \int \frac{d^4k}{(2\pi)^4}\, \frac{1}{N_0 N_1 N_2 N_3 N_4}, \tag{4}$$

where

$$N_0 = k^2 - \lambda^2 + io \quad \text{and} \quad N_i = (k+p_i)^2 - m_i^2 + io. \tag{5}$$

Here io denotes an infinitesimal imaginary part. The plus sign accompanying this imaginary part is determined by causality. The mass parameter λ is in principle arbitrary. In our case, however, it will denote a non-zero photon mass, needed for regularizing the infrared divergences.

Before starting with the decomposition, we first derive a useful identity. To this end we exploit Lorentz covariance and write

$$\int \frac{d^4k}{(2\pi)^4}\,\frac{k^\mu}{N_0N_1N_2N_3} = c_1\,p_1^\mu + c_2\,p_2^\mu + c_3\,p_3^\mu. \tag{6}$$

The integral on the left-hand side is ultraviolet-finite and, when properly regularized, also infrared-finite. The quantities c_i on the right-hand side are therefore finite coefficients, dependent on masses and the invariants $p_i \cdot p_j$ $(i,j = 1,2,3)$. Contracting this expression with the antisymmetric Levi–Civita tensor, one obtains the identity

$$\int \frac{d^4k}{(2\pi)^4}\,\frac{\varepsilon_{p_1p_2p_3k}}{N_0N_1N_2N_3} = 0, \tag{7}$$

where we introduced the widely-used notation

$$\varepsilon_{\mu\nu\rho p} = \varepsilon_{\mu\nu\rho\sigma}p^\sigma, \quad \varepsilon_{\mu\nu pq} = \varepsilon_{\mu\nu\rho\sigma}p^\rho q^\sigma, \ \cdots \tag{8}$$

In our convention, the Levi–Civita tensor is defined according to $\varepsilon^{0123} = -\varepsilon_{0123} = 1$. The above identity will prove extremely useful in the following.

The actual derivation of the decomposition formula starts with the Schouten identity

$$a\,k^\mu = \sum_{i=1}^{4} v_i^\mu\,(p_i \cdot k), \tag{9}$$

where the following notation was used:

$$v_1^\mu = \varepsilon^{\mu p_2p_3p_4}, \quad v_2^\mu = \varepsilon^{p_1\mu p_3p_4}, \quad v_3^\mu = \varepsilon^{p_1p_2\mu p_4}, \quad v_4^\mu = \varepsilon^{p_1p_2p_3\mu}, \quad a = \varepsilon_{p_1p_2p_3p_4} = \varepsilon^{p_1p_2p_3p_4}. \tag{10}$$

Note that from the quantity a one can construct the Gram-determinant of the system, $\Delta_4 = a^2$. The next step in the derivation is to contract the Schouten identity with k_μ, yielding

$$a\,k^2 = \sum_{i=1}^{4}(k \cdot v_i)(k \cdot p_i). \tag{11}$$

Now we can substitute

$$\begin{aligned} k^2 &= N_0 + \lambda^2 - io, \\ (k \cdot p_i) &= \frac{1}{2}\,[N_i - N_0 - r_i], \quad \text{with} \quad r_i = p_i^2 - m_i^2 + \lambda^2 \end{aligned} \tag{12}$$

to arrive at

$$2a\,(N_0 + \lambda^2) = \sum_{i=1}^{4}(k \cdot v_i)(N_i - N_0 - r_i). \tag{13}$$

In order to make the link to the scalar five-point function, one should divide this expression by $N_0N_1N_2N_3N_4$ and perform the integration over d^4k. As a result of Eq. (7) the N_i terms vanish. The terms $\sum(k \cdot v_i)\,N_0$ can be transformed according to

$$\sum_{i=1}^{4}(k \cdot v_i) = \varepsilon^{(k+p_1)(p_2-p_1)(p_3-p_1)(p_4-p_1)} - a, \tag{14}$$

which can be verified by a direct check. After integration the first term will vanish. This can be most easily seen by making a change of integration variable, $\tilde{k}^\mu = k^\mu + p_1^\mu$, and subsequently applying Eq. (7). The complete expression now reads

$$\int \frac{d^4k}{(2\pi)^4} \frac{aN_0 + 2a\lambda^2 + \sum r_i (k \cdot v_i)}{N_0 N_1 N_2 N_3 N_4} = 0. \tag{15}$$

The final step is to multiply this expression by a and to apply the Schouten identity and Eq. (12) to the last term in the numerator. This allows us to express the complete numerator in terms of the propagators appearing in the denominator:

$$\int \frac{d^4k}{(2\pi)^4} \frac{2\lambda^2\Delta_4 - \frac{1}{2}w^2 + N_0\Delta_4 - \frac{1}{2}N_0 \sum (v_i \cdot w) + \frac{1}{2}\sum N_i (v_i \cdot w)}{N_0 N_1 N_2 N_3 N_4} = 0, \tag{16}$$

with

$$w^\mu = \sum_{j=1}^{4} r_j \, v_j^\mu . \tag{17}$$

The final formula for the decomposition reads

$$\begin{aligned} (w^2 - 4\lambda^2\Delta_4)\, E_{01234} &= (w \cdot v_1)\, D_{0234} + (w \cdot v_2)\, D_{0134} + (w \cdot v_3)\, D_{0124} + (w \cdot v_4)\, D_{0123} \\ &\quad + \left[2\Delta_4 - \sum_{i=1}^{4} (w \cdot v_i) \right] D_{1234}, \end{aligned} \tag{18}$$

where D_{0234}, D_{0134}, etc., denote four-point scalar functions containing the propagators with labels $(0,2,3,4)$, $(0,1,3,4)$, etc.

The generalization of this decomposition to higher multipoint functions can be performed in a similar way [11]. In general, a scalar N-point function can be expressed in terms of the N underlying $(N-1)$-point functions.

2.2 Decomposition of the real five-point function

Using the derivation presented in the previous subsection as guideline, we can now try to derive a similar decomposition for the real five-point function. As can be read off from Fig. 1, by taking the exchanged photon to be on-shell, the real five-point function takes the form

$$E^{\mathrm{R}}_{01234} = \int \frac{d^3k}{(2\pi)^3\, 2\omega} \frac{1}{N_1' N_2' N_3' N_4'}, \tag{19}$$

where

$$\omega = \sqrt{\vec{k}^2 + \lambda^2}\,, \quad N_{1,2}' = N_{1,2}, \quad \text{and} \quad N_{3,4}' = N_{3,4}^*. \tag{20}$$

The photon is now on-shell, so $k^2 = \lambda^2$ and $N_0 = 0$. Note that the momenta p_i, hidden inside N_i, are time-like and have positive energy components.

One can proceed in the same way as in the case of the decomposition of the virtual five-point function. The Schouten identity is still valid, but Eq. (7) in its old form does not work in the case of real-photon radiation, and should be modified. In the derivation of the virtual decomposition, Eq. (7) was used twice, leading to the nullification of

$$\int \frac{d^4k}{(2\pi)^4} \frac{\sum(k\cdot v_i) N_i}{N_0 N_1 N_2 N_3 N_4} \quad \text{and} \quad \int \frac{d^4k}{(2\pi)^4} \frac{N_0\left[\sum(k\cdot v_i)+a\right]}{N_0 N_1 N_2 N_3 N_4}. \tag{21}$$

In the case of real-photon radiation, this will correspond to

$$\int \frac{d^3k}{(2\pi)^3\, 2\omega} \frac{\sum(k\cdot v_i)\, N_i'}{N_1' N_2' N_3' N_4'} \quad \text{and} \quad \int \frac{d^3k}{(2\pi)^3\, 2\omega} \frac{N_0\left[\sum(k\cdot v_i)+a\right]}{N_1' N_2' N_3' N_4'}. \tag{22}$$

For the nullification of the second integral the validity of Eq. (7) is immaterial, since for the on-shell photon $N_0 = 0$ anyway. The first integral, however, is no longer necessarily zero. The fact that the photon is on-shell implies that $k^2 = \lambda^2$ and that the propagators N_i are linear in k. By simple power counting, one can conclude that this integral is formally ultraviolet-divergent. For this reason, the Lorentz-covariance argument used in Eq. (6) is not correct any more and Eq. (7) is invalidated.

Apart from the modification of Eq. (7) and the fact that $N_0 = 0$, the derivation of the decomposition for the real five-point function is not changed, resulting in

$$\begin{aligned}(w^2 - 4\lambda^2\Delta_4)\, E^{\mathrm{R}}_{01234} \;&=\; (w\cdot v_1)\, D^{\mathrm{R}}_{0234} + (w\cdot v_2)\, D^{\mathrm{R}}_{0134} + (w\cdot v_3)\, D^{\mathrm{R}}_{0124} + (w\cdot v_4)\, D^{\mathrm{R}}_{0123} \\ &\quad - 2\int \frac{d^3k}{(2\pi)^3\, 2\omega} \frac{\sum a\,(k\cdot v_i)\, N_i'}{N_1' N_2' N_3' N_4'}.\end{aligned} \tag{23}$$

The main difference with the virtual decomposition is the occurrence of the last term in Eq. (23). It turns out that the poles in this particular integral can be moved in such a way that $N_i' \to N_i$ for all i. Indeed, the integral can be rewritten in the following way:

$$\int \frac{d^3k}{(2\pi)^3\, 2\omega} \frac{\sum(k\cdot v_i)\, N_i'}{N_1' N_2' N_3' N_4'} = \int \frac{d^3k}{(2\pi)^3\, 2\omega} \frac{\sum(k\cdot v_i)\, N_i}{N_1 N_2 N_3 N_4} + \Delta^{(1)} + \Delta^{(2)}, \tag{24}$$

with

$$\begin{aligned}\Delta^{(1)} \;&=\; \int \frac{d^3k}{(2\pi)^3\, 2\omega} \frac{(k\cdot v_1)\, N_1 + (k\cdot v_2)\, N_2}{N_1 N_2} \Big[\frac{1}{N_3' N_4'} - \frac{1}{N_3 N_4}\Big], \\ \Delta^{(2)} \;&=\; \int \frac{d^3k}{(2\pi)^3\, 2\omega} \left\{ \frac{(k\cdot v_3)}{N_1 N_2}\Big[\frac{1}{N_4'} - \frac{1}{N_4}\Big] + \frac{(k\cdot v_4)}{N_1 N_2}\Big[\frac{1}{N_3'} - \frac{1}{N_3}\Big] \right\}.\end{aligned} \tag{25}$$

Both $\Delta^{(1)}$ and $\Delta^{(2)}$ are in fact zero. Let us consider, for example, one of the terms contributing to $\Delta^{(2)} = \Delta^{(2)}_3 + \Delta^{(2)}_4$, e.g.

$$\Delta^{(2)}_4 = \int \frac{d^3k}{(2\pi)^3\, 2\omega} \frac{(k\cdot v_4)}{N_1 N_2} \frac{2i\,\mathrm{Im}\, N_3}{N_3 N_3'}. \tag{26}$$

This integral is ultraviolet-finite, even for an on-shell photon, and therefore no regularization is needed. Consequently, the Lorentz-covariance argument is valid:

$$\int \frac{d^3k}{2\omega}\,\frac{k^\mu}{N_1N_2N_3N_3'} = c_1\,p_1^\mu + c_2\,p_2^\mu + c_3\,p_3^\mu, \tag{27}$$

where the quantities c_i are finite coefficients. Contracting the last expression with $v_{4\,\mu} = \varepsilon_{p_1p_2p_3\mu}$, one arrives at $\Delta_4^{(2)} = 0$. Using similar arguments one can prove that $\Delta^{(1)} = \Delta^{(2)} = 0$.

An important point in this line of reasoning was the use of Lorentz-invariance of the integration d^3k/ω. Such an integration is indeed Lorentz-invariant, provided that the area of integration is Lorentz-invariant. In the context of the double-pole approximation, the photon is treated inclusively, with the integration performed over all possible values of k up to infinity. If one would, however, consider an exclusive process, involving the introduction of a cutoff Ω_{max}, then the area of integration might fail to be Lorentz-invariant, and the decomposition stops at Eq.(23). In order to successfully proceed beyond that point for exclusive processes, one should make sure that the cut-off prescription, which defines the area of integration, does not introduce new independent four-vectors in the integral. If this condition is satisfied, a generalization of the decomposition to exclusive bremsstrahlung processes should be feasible.

So, in our approach, the following identity has been established:

$$\int \frac{d^3k}{(2\pi)^3\,2\omega}\,\frac{\sum(k\cdot v_i)\,N_i'}{N_1'N_2'N_3'N_4'} = \int \frac{d^3k}{(2\pi)^3\,2\omega}\,\frac{\sum(k\cdot v_i)\,N_i}{N_1N_2N_3N_4}. \tag{28}$$

As was already noted, the integral on the right-hand side is formally divergent. Its virtual analogue, being formally finite, vanishes:

$$\int \frac{d^4k}{(2\pi)^4}\,\frac{\sum(k\cdot v_i)\,N_i}{N_0N_1N_2N_3N_4} = 0. \tag{29}$$

Performing a contour integration in the lower half of the complex k_0-plane, indicated by the integration contour C_O in Fig. 3, one can use this identity to relate the photon-pole contribution to the particle-pole contributions:

$$-\,2\pi i \int \frac{d^3k}{(2\pi)^4\,2\omega}\,\frac{\sum(k\cdot v_i)N_i}{N_1N_2N_3N_4} = -\int \frac{d^4k}{(2\pi)^4 N_0}\,\mathcal{P}ole\,\frac{\sum(k\cdot v_i)N_i}{N_1N_2N_3N_4}. \tag{30}$$

Here "$\mathcal{P}ole$" denotes the complex particle poles that should be taken into account. Note that the left-hand side of Eq. (30) corresponds to the real-photon radiation integral that we are pursuing to evaluate. The integral on the right-hand side does not correspond to on-shell photons any more, since $N_0 \neq 0$. Now we can use the Schouten identity to substitute

$$\sum_{i=1}^{4}(k\cdot v_i)\,N_i = \sum_{i=1}^{4}(k\cdot v_i)\,N_0 + 2ak^2 + \sum_{i=1}^{4} r_i\,(k\cdot v_i) \tag{31}$$

on the right-hand side. After some rearrangements one obtains

$$2\pi i \int \frac{d^3k}{(2\pi)^4\,2\omega}\,\frac{\sum(k\cdot v_i)\,N_i}{N_1N_2N_3N_4} = \int \frac{d^4k}{(2\pi)^4}\,\frac{\sum(k\cdot v_i)+2a}{N_1N_2N_3N_4} + \int \frac{d^4k}{(2\pi)^4 N_0}\,\mathcal{P}ole\,\frac{\sum r_i\,(k\cdot v_i)+2a\lambda^2}{N_1N_2N_3N_4}. \tag{32}$$

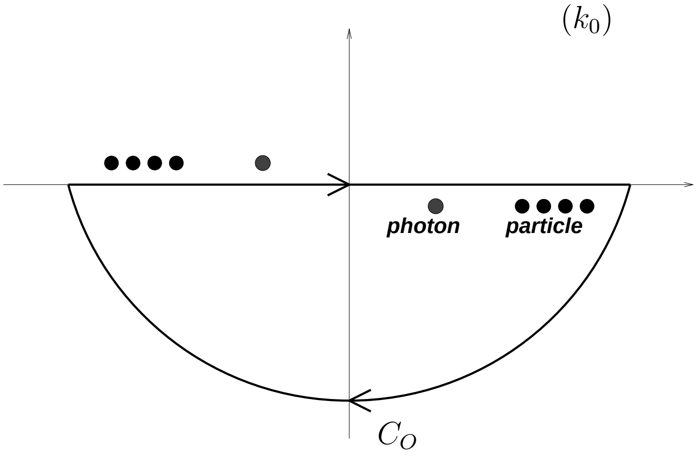

Figure 3: Integration contour in the lower half of the complex k_0-plane leading to Eq. (30).

The first integral on the right-hand side can be simplified with the help of Eqs. (14) and (7), yielding

$$2\pi i \int \frac{d^3k}{(2\pi)^4\, 2\omega} \frac{\sum (k\cdot v_i)\, N_i}{N_1 N_2 N_3 N_4} = a \int \frac{d^4k}{(2\pi)^4} \frac{1}{N_1 N_2 N_3 N_4} + \mathcal{R}, \tag{33}$$

with

$$\mathcal{R} = \int \frac{d^4k}{(2\pi)^4 N_0}\, \mathcal{P}ole\, \frac{\sum r_i\,(k\cdot v_i) + 2a\lambda^2}{N_1 N_2 N_3 N_4}. \tag{34}$$

In App. B it is shown that the $\mathcal{R}$ term in (33), which consists of a combination of particle-pole contributions, vanishes. After that the decomposition for the real five-point function can be written in a compact form, analogous to the decomposition of the virtual five-point function

$$\begin{aligned}(w^2 - 4\lambda^2\Delta_4)\, E^{\mathrm{R}}_{01234} \;\; &= \;\; (w\cdot v_1)\, D^{\mathrm{R}}_{0234} + (w\cdot v_2)\, D^{\mathrm{R}}_{0134} + (w\cdot v_3)\, D^{\mathrm{R}}_{0124} + (w\cdot v_4)\, D^{\mathrm{R}}_{0123} \\ &\quad + 2i\Delta_4 \int \frac{d^4k}{(2\pi)^4} \frac{1}{N_1 N_2 N_3 N_4}.\end{aligned} \tag{35}$$

Note that the last term on the right-hand side of Eq. (35) is exactly a virtual scalar four-point function with a coefficient $2i\Delta_4$. In comparing Eq. (18) to Eq. (35) one observes certain similarities: the first four terms in Eq. (35) are the radiative analogues of their virtual counterparts in Eq. (18). One may naively think that the last term in (35) should not be there, since it does not correspond to photon radiation. In fact, it is a direct consequence of having ultraviolet-divergent integrals during the intermediate steps of the derivation.

This concludes the derivation of the decomposition of the five-point function corresponding to inclusive bremsstrahlung. As was noted before, generalization to the case of exclusive bremsstrahlung is possible, provided that the cut-off is introduced in such a way that no new independent four-vectors appear in the integrals. In analogy to what was remarked for the virtual decomposition, also the generalization to higher multipoint radiation functions is possible and rather straightforward. One should simply follow the approach of Ref. [11] for multipoint scalar functions.

2.3 Application of the five-point decompositions

We can now apply the five-point decompositions to the non-factorizable W-pair corrections. The virtual scalar five-point function, corresponding to the third diagram in Fig. 1, reads in the double-pole approximation

$$w^2\, E_{01234} = 2\Delta_4\, D_{1234} + (w\cdot v_1)\, D_{0234} + (w\cdot v_2)\, D_{0134} + (w\cdot v_3)\, D_{0124} + (w\cdot v_4)\, D_{0123}, \qquad (36)$$

with

$$\begin{aligned} v_{1\mu} &= -\,\varepsilon_{\mu p_2 k_1 k_2}, \qquad v_{2\mu} = +\,\varepsilon_{p_1 \mu k_1 k_2}, \qquad v_{3\mu} = -\,\varepsilon_{p_1 p_2 \mu k_2}, \\ v_{4\mu} &= +\,\varepsilon_{p_1 p_2 k_1 \mu}, \qquad w^\mu = D_1 v_1^\mu + D_2 v_2^\mu, \qquad \Delta_4 = [\,\varepsilon_{p_1 p_2 k_1 k_2}\,]^2. \end{aligned} \qquad (37)$$

Comparison with Eq. (18) reveals that the terms $-\sum (w\cdot v_i)\, D_{1234}$ have been neglected, since they are formally of higher order in the expansion in powers of Γ_W/M_W. Note that the scalar four-point function D_{1234} is purely a consequence of the decomposition (36). It does not involve the exchange of a photon and is therefore not affected by the soft-photon approximation. Since the factor $2\Delta_4/w^2$ is already doubly resonant, D_{1234} should be calculated for on-shell W bosons. The scalar four-point functions D_{0134} and D_{0234} are infrared-divergent and should be calculated in the soft-photon approximation.

In the same way, the five-point function corresponding to real-photon radiation is given by

$$w'^2\, E^{\rm R}_{01234} = 2i\Delta_4\, D^{\rm R}_{1234} + (w'\cdot v'_1)\, D^{\rm R}_{0234} + (w'\cdot v'_2)\, D^{\rm R}_{0134} + (w'\cdot v'_3)\, D^{\rm R}_{0124} + (w'\cdot v'_4)\, D^{\rm R}_{0123}. \qquad (38)$$

The four-vectors w' and v'_i are defined as before, but for real-photon emission. This is equivalent to the following substitutions: $p_1 \to -p_1$, $k_1 \to -k_1$ and $D_2 \to D_2^*$. The radiation function $D^{\rm R}_{1234}$ is an artefact of the decomposition (38) and does not involve the exchange of a photon. It can be obtained from D_{1234} by the substitutions $p_1 \to -p_1$ and $k_1 \to -k_1$. In the double-pole approximation, i.e. for on-shell W bosons, this implies the relation $D^{\rm R}_{1234} = i{\rm Im}\, D_{1234}$. This property ensures the cancellation of the virtual non-factorizable D_{1234}-dependent corrections against the corresponding real-photon corrections, provided that the integration over the W-boson virtualities (i.e. $D_{1,2}$) is performed. This phenomenon is a general consequence of the soft-photon approximation [5].

2.4 Connection between virtual and real contributions

At this point we have reduced the calculation of the non-factorizable corrections to the evaluation of virtual and real four-point functions. We can, however, go one step further and establish a connection between the contribution from the photon-pole part of the virtual scalar functions, D^{γ}, and the corresponding radiative interferences. To this end, we consider for example the contributions related to D^{γ}_{0123} and D^{R}_{0123}. The contribution of the radiative interference to the cross-section (see Fig. 1) is given by

$$d\sigma_{\mathrm{real}}(D^{\mathrm{R}}_{0123}) = d\sigma_{\mathrm{Born}}\,\mathrm{Re}\int \frac{d^3k}{(2\pi)^3\,2\omega}\,\frac{32\pi\alpha\,(p_2\cdot k_1)\,D_1}{[D_1+2(p_1\cdot k)][D_2^*+2(p_2\cdot k)][2(k_1\cdot k)+io]}, \tag{39}$$

where $k_0 = \omega = |\vec{k}|$.

This has to be compared with the corresponding photon-pole part of the virtual correction. This contribution is evaluated in the lower half of the complex k_0-plane, where the photon pole is situated at $k_0 = \omega = |\vec{k}| - io$:

$$d\sigma_{\mathrm{virt}}(D^{\gamma}_{0123}) = d\sigma_{\mathrm{Born}}\,\mathrm{Re}\int \frac{d^3k}{(2\pi)^3\,2\omega}\,\frac{32\pi\alpha\,(p_2\cdot k_1)\,D_1}{[D_1-2(p_1\cdot k)][D_2+2(p_2\cdot k)][-2(k_1\cdot k)+io]}. \tag{40}$$

This can be rewritten in the form

$$d\sigma_{\mathrm{virt}}(D^{\gamma}_{0123}) = d\sigma_{\mathrm{Born}}\,\mathrm{Re}\int \frac{d^3k}{(2\pi)^3\,2\omega}\,\frac{32\pi\alpha\,(p_2\cdot k_1)\,D_1^*}{[D_1^*-2(p_1\cdot k)][D_2^*+2(p_2\cdot k)][-2(k_1\cdot k)-io]}. \tag{41}$$

Comparing Eqs. (39) and (41), one can readily see that $d\sigma_{\mathrm{real}}(D^{\mathrm{R}}_{0123})$ can be obtained from the photon-pole contribution to the virtual correction $d\sigma_{\mathrm{virt}}(D^{\gamma}_{0123})$, by adding an overall minus sign and substituting[2] $D_1 \to -D_1^*$. In a similar way $d\sigma_{\mathrm{real}}(D^{\mathrm{R}}_{0124})$ can be obtained from the photon-pole contribution to the virtual correction $d\sigma_{\mathrm{virt}}(D^{\gamma}_{0124})$, by adding an overall minus sign and substituting $D_2 \to -D_2^*$. The different substitution rule reflects the fact that we will determine D_{0124} and D^{γ}_{0124} from D_{0123} and D^{γ}_{0123} by substituting $(p_1,k_1) \leftrightarrow (p_2,k_2)$. Note that this is equivalent to evaluating D^{γ}_{0124} in the upper half of the complex k_0-plane.

Also the "Coulomb" and five-point contributions can be treated in this way, bearing in mind that the coefficients of the five-point decomposition also depend on $D_{1,2}$. In conclusion, the following relation emerges. The radiative interferences can be obtained from Eqs. (2) and (3) by adding a minus sign, by inserting the decomposition given in Eq. (36), and by substituting

– in the D_{0123}, D_{0134} terms: $D_{0123}, D_{0134} \to D^{\gamma}_{0123}, D^{\gamma}_{0134}$ followed by $D_1 \to -D_1^*$,
– in the D_{0124}, D_{0234} terms: $D_{0124}, D_{0234} \to D^{\gamma}_{0124}, D^{\gamma}_{0234}$ followed by $D_2 \to -D_2^*$,
– in the D_{1234} terms: $D_{1234} \to D^{\mathrm{R}}_{1234}$ followed by $D_2 \to -D_2^*$,
– in the C_{012} terms: $C_{012} \to C^{\gamma}_{012}$ followed by $D_1 \to -D_1^*$.

Here both D^{γ}_{0124} and D^{γ}_{0234} are determined by substituting $(p_1,k_1) \leftrightarrow (p_2,k_2)$ in the expressions for D^{γ}_{0123} and D^{γ}_{0134}, respectively. As such, the above connection between real and virtual corrections implies that D^{γ}_{0124} and D^{γ}_{0234} are evaluated in the upper half-plane.

---

[2] Note that $d\sigma_{\mathrm{Born}}$ is not affected by substitutions of the form $D_i \to -D_i^*$ $(i=1,2)$, since it only depends on $|D_1D_2|^2$.

Note that the above-presented connection between the virtual and real non-factorizable corrections hinges on two things. First of all, the inclusive treatment of the bremsstrahlung photon, with the phase-space integration extending to infinity. Second, the fact that both virtual and real corrections are calculated in the soft-photon approximation, inherent in the double-pole approach.

As mentioned before, manifestly non-factorizable initial–final state interference effects are also possible in our approach. As stated in Sect. 1.1 we will now briefly indicate why these effects vanish. Let us consider, for example, the initial–final state interference contribution corresponding to the photonic interaction between the positron $[e^+(q_1)]$ and the positively charged final-state lepton $[\ell^+(k_1)]$. In the soft-photon approximation, the contribution of the virtual interference to the cross-section is

$$d\sigma_{\rm virt}(D_{if}) = -d\sigma_{\rm Born}\,{\rm Re}\int\frac{d^4k}{(2\pi)^4}\,\frac{32i\pi\alpha\,(q_1\cdot k_1)\,D_1}{[k^2-\lambda^2+io][D_1-2(p_1\cdot k)][-2(k_1\cdot k)+io][-2(q_1\cdot k)+io]}. \tag{42}$$

Note that all particle poles are situated in the upper half of the complex k_0-plane. By closing the integration contour in the lower half-plane, one finds that the complete virtual correction is equal to the photon-pole contribution

$$d\sigma_{\rm virt}(D_{if}) = -d\sigma_{\rm Born}\,{\rm Re}\int\frac{d^3k}{(2\pi)^3\,2\omega}\,\frac{32\pi\alpha\,(q_1\cdot k_1)\,D_1}{[D_1-2(p_1\cdot k)][-2(k_1\cdot k)+io][-2(q_1\cdot k)+io]}, \tag{43}$$

with $k_0=\omega=\sqrt{\vec{k}^2+\lambda^2-io}$. On the other hand, the corresponding bremsstrahlung interference can be written as

$$d\sigma_{\rm real}(D_{if}^{\rm R}) = -d\sigma_{\rm Born}\,{\rm Re}\int\frac{d^3k}{(2\pi)^3\,2\omega}\,\frac{32\pi\alpha\,(q_1\cdot k_1)\,D_1^*}{[D_1^*+2(p_1.k)][2(k_1\cdot k)-io][-2(q_1\cdot k)+io]}. \tag{44}$$

By comparing the last two expressions, one can readily derive that the virtual and real interferences only differ by an overall minus sign and the substitution $D_1\to -D_1^*$. In the next section we derive an explicit expression for infrared-divergent virtual scalar four-point functions [see Eq.(72)].[3] From this expression one can see that the substitution $D_1\to -D_1^*$ does not change the real part of the interference (42), i.e. the sum of virtual and real interferences gives rise to a vanishing non-factorizable correction. Analogously, no other non-factorizable initial–final and initial–intermediate state photonic interferences contribute to the double resonant cross-section, if both virtual and real corrections are included. Similar arguments can be used to prove that initial-state up–down QED interferences vanish in our approach.

---

[3] In our example we need Eq. (72) with k_2 replaced by $-q_1$. Note that, as a result of this substitution, the invariant s_{12} becomes negative.

3 Modified standard technique: Feynman-parameter integrals

In this section we present the calculation of the relevant virtual scalar functions, using Feynman-parameter integrals. In addition the photon-pole parts of these functions are given, from which the real-photon corrections can be extracted. The striking difference with the usual calculations of scalar integrals lies in the systematic application of the soft-photon approximation.

3.1 Scalar four-point functions in the soft-photon approximation

In this subsection we illustrate how to calculate a virtual scalar four-point function in the soft-photon approximation and how to extract the photon-pole part. Consider to this end

$$D_{\rm virt} = \int \frac{d^4k}{(2\pi)^4}\,\frac{1}{[k^2+io][2(p_1\cdot k)+D_1+io][2(p_2\cdot k)+D_2+io][2(p_3\cdot k)+D_3+io]}, \tag{45}$$

where $D_i = p_i^2 - M_i^2$. In general, the energy components p_i^0 of the arbitrary momenta p_i are not necessarily positive. In contrast to the usual Feynman-parameter technique, where the Feynman-parameter transformation is applied to all propagators, we apply it only to propagators that are linear in k:

$$D_{\rm virt} = 2\int_0^1 d^3\xi\,\delta\Bigl(1-\sum_{i=1}^3 \xi_i\Bigr)\, I_{\rm virt}(\xi), \tag{46}$$

with

$$I_{\rm virt}(\xi) = \int \frac{d^4k}{(2\pi)^4}\,\frac{1}{[k_0^2-\vec{k}^2+io][k_0E(\xi)-\vec{k}\cdot\vec{p}(\xi)+A(\xi)+io]^3}. \tag{47}$$

The quantities $A(\xi)$ and $p^\mu(\xi)$ are given by

$$A(\xi) = \sum_{i=1}^3 \xi_i\, D_i \quad\text{and}\quad p^\mu(\xi) = 2\sum_{i=1}^3 \xi_i\, p_i^\mu. \tag{48}$$

The energy component $E(\xi)$ of $p^\mu(\xi)$ can be positive or negative. However, there is a freedom to choose $E(\xi)\le 0$, because one can always perform a transformation of variables $k_0 \to -k_0$. Then

$$I_{\rm virt}(\xi) = \int \frac{d^4k}{(2\pi)^4}\,\frac{1}{[k_0^2-\vec{k}^2+io][-k_0|E(\xi)|-\vec{k}\cdot\vec{p}(\xi)+A(\xi)+io]^3}. \tag{49}$$

In the complex k_0-plane the denominators give rise to poles. There are two photon poles, one in the upper and one in the lower half-plane. The second denominator gives rise to a "particle" pole in the upper half-plane, for any value of ξ_i. It should be noted that this combines the three particle poles present in (45), which could lie in the upper or lower half-plane. Closing the integration contour in the lower half-plane we get

$$I_{\rm virt}(\xi) = -i\int \frac{d^3k}{(2\pi)^3}\,\frac{1}{2\,|\vec{k}|\,(-|\vec{k}|\,|E(\xi)|-x|\vec{k}|\,|\vec{p}(\xi)|+A(\xi)+io)^3}, \tag{50}$$

where $x = \cos\theta$, with θ being the angle between $\vec{p}(\xi)$ and $\vec{k}$. It is not very difficult to perform the rest of the integrations in momentum space. The final result is

$$I_{\rm virt}(\xi) = -\frac{i}{8\pi^2}\,\frac{1}{A(\xi)\,(p^2(\xi) - io|E(\xi)|)}. \tag{51}$$

As we have seen in the previous section, the real-photon radiative interferences can be obtained from the photon-pole parts of the virtual corrections. Let us therefore consider the photon-pole part of (45) in the lower half of the complex k_0-plane:

$$D^{\gamma}_{\rm virt} = -i\int\frac{d^3k}{(2\pi)^3}\,\frac{1}{2\,|\vec{k}|\,[2(p_1\cdot k) + D_1 + io][2(p_2\cdot k) + D_2 + io][2(p_3\cdot k) + D_3 + io]}, \tag{52}$$

with $k_0 = \sqrt{\vec{k}^2 - io}$. One can again proceed by introducing the Feynman parameters to obtain

$$I^{\gamma}_{\rm virt}(\xi) = -i\int\frac{d^3k}{(2\pi)^3}\,\frac{1}{2\,|\vec{k}|\,\Big[E(\xi)\,\sqrt{\vec{k}^2 - io} - x\,|\vec{k}|\,|\vec{p}(\xi)| + A(\xi) + io\Big]^3}. \tag{53}$$

Equations (50) and (53) are the same up to small modifications. In the case of the full virtual scalar function, Eq. (50) was obtained after contour integration in the complex k_0-plane. In that case we had the freedom to choose the contour in such a way that $E(\xi) \le 0$. Now we have no such freedom. So, $E(\xi)$ cannot be considered as a negative quantity any more. It is clear that the final answer will be

$$I^{\gamma}_{\rm virt}(\xi) = -\frac{i}{8\pi^2}\,\frac{1}{A(\xi)\,[p^2(\xi) + ioE(\xi)]}. \tag{54}$$

This expression is very similar to the one derived for the full virtual scalar function. It can in fact be rewritten as

$$I^{\gamma}_{\rm virt}(\xi) = -\frac{i}{8\pi^2}\,\frac{1}{A(\xi)}\left\{\frac{1}{p^2(\xi) - io|E(\xi)|} - 2i\pi\,\theta[E(\xi)]\,\delta[p^2(\xi)]\right\}, \tag{55}$$

where the first term in the curly brackets corresponds to the full virtual scalar function and the second term is the necessary modification. The second term in Eq. (55) is the analogue of the "particle"-pole contribution in the approach of [9]. Note that this term has an extra factor i. If all quantities were to be real (stable-particle case), then this term would not contribute to the non-factorizable correction to the cross-section, for which only the real part is important. In the case of unstable particles, this "particle"-pole contribution is felt by the imaginary parts of the W-boson propagators, resulting in a potentially non-zero contribution to the cross-section. If one were to evaluate the photon-pole part of (45) in the upper half of the complex k_0-plane, one merely would have to replace $E(\xi)$ by $-E(\xi)$ in Eqs. (54) and (55).

In practice, we calculate the relevant four-point functions $D_{\rm virt}$ as well as the corresponding particle-pole contributions $D^{\rm part}_{\rm virt}$. The photon-pole part $D^{\gamma}_{\rm virt}$ is obtained as $D^{\gamma}_{\rm virt} = D_{\rm virt} - D^{\rm part}_{\rm virt}$, which can then be used to evaluate the real-photon radiative interferences. The complex half-plane where the particle-pole (photon-pole) contributions should be evaluated is fixed according to the rules given in Sect. 2.4.

3.2 Calculation of the virtual scalar four-point functions

In this subsection we present the calculation of the virtual scalar four-point functions and the associated photon-pole parts. Everything is considered in the soft-photon approximation. Since the four-point function D_{1234} does not involve this approximation, we defer the corresponding results to App. A.1 and merely refer to the literature [12, 13] for its derivation.

Before listing the various results, we define our notation. To write down the analytical results we need to introduce some kinematic invariants:

$$\begin{aligned} &m_{1,2}^2 = k_{1,2}^2, \quad s = (p_1+p_2)^2, \quad s_{12} = (k_1+k_2)^2, \\ &s_{211'} = (k_2+k_1+k_1')^2, \quad s_{122'} = (k_1+k_2+k_2')^2, \end{aligned} \tag{56}$$

and some short-hand notations:

$$\begin{aligned} &y_0 = \frac{D_1}{D_2}, \quad x_s = \frac{\beta-1}{\beta+1} + io, \quad \beta = \sqrt{1-4M_W^2/s}\,, \\ &\zeta = 1 - \frac{s_{122'}}{M_W^2} - io, \quad \zeta' = 1 - \frac{s_{211'}}{M_W^2} - io\,. \end{aligned} \tag{57}$$

3.2.1 The virtual infrared-finite four-point function

We start off with the calculation of the infrared-finite scalar four-point function D_{0123}, which corresponds to the first diagram shown in Fig. 1. This function is infrared-finite owing to the presence of finite decay widths in the propagators of the unstable W bosons. In the soft-photon limit we find

$$D_{0123} = \int \frac{d^4k}{(2\pi)^4} \, \frac{1}{[k^2+io][D_1 - 2(p_1\cdot k)][D_2 + 2(p_2\cdot k)][-2(k_1\cdot k)+io]}, \tag{58}$$

where $D_{1,2} = p_{1,2}^2 - M_W^2 + io$. Originally the quantities $D_{1,2}$ are real, with the usual infinitesimal imaginary part. At the end of the calculation the analytical continuation to finite imaginary parts can be performed. Then $D_{1,2} = p_{1,2}^2 - M_W^2 + iM_W\Gamma_W$.

Applying the Feynman-parameter technique as explained in Sect. 3.1, we obtain the following representation

$$D_{0123} = \frac{-i}{4\pi^2} \int_0^1 d^3\xi \, \delta\Big(1 - \sum_{i=1}^{3} \xi_i\Big) \, \frac{1}{A(\xi)\,[p^2(\xi) - io]} \tag{59}$$

with

$$A(\xi) = \xi_1\, D_1 + \xi_2\, D_2, \quad p^\mu(\xi) = -2\xi_1\, p_1^\mu + 2\xi_2\, p_2^\mu - 2\xi_3\, k_1^\mu. \tag{60}$$

As was indicated before, the integral will be calculated for small final-state fermion masses and in the double-pole approximation. This implies

$$2(p_1\cdot k_1) \approx p_1^2 \approx M_W^2 \quad \text{and} \quad 2(p_2\cdot k_2) \approx p_2^2 \approx M_W^2. \tag{61}$$

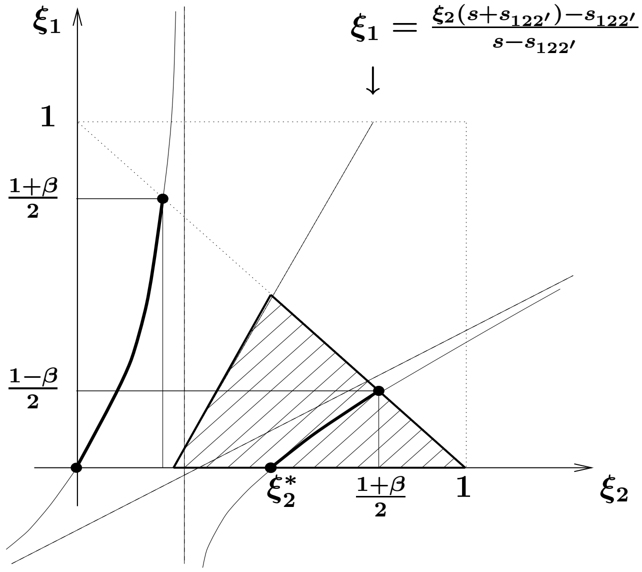

Figure 4: The integration area (shaded region) in the (ξ_1, ξ_2) Feynman-parameter space for the calculation of the particle-pole part D_{0123}^{part} of the infrared-finite scalar four-point function D_{0123}. The thicker curves indicate the solutions of $p^2(\xi) = 0$, with $\xi_2^* = 1 - M_W^2/s_{122'}$.

What is left is the integral over the space of Feynman parameters. The details of the integration are presented in App. A.2. The final answer reads

$$\begin{aligned} D_{0123} \;\; = \;\; & \frac{i}{16\pi^2 M_W^2}\,\frac{1}{[D_2-\zeta D_1]}\biggl\{2\,\mathcal{L}\mathrm{i}_2\Bigl(\frac{1}{y_0};\frac{1}{\zeta}\Bigr) - \mathcal{L}\mathrm{i}_2\Bigl(x_s;\frac{1}{y_0}\Bigr) - \mathcal{L}\mathrm{i}_2\Bigl(\frac{1}{x_s};\frac{1}{y_0}\Bigr) \\ & + \mathcal{L}\mathrm{i}_2\Bigl(x_s;\zeta\Bigr) + \mathcal{L}\mathrm{i}_2\Bigl(\frac{1}{x_s};\zeta\Bigr) + \Bigl[\ln\Bigl(\frac{M_W^2}{m_1^2}\Bigr) + 2\ln(\zeta)\Bigr]\Bigl[\ln(y_0) + \ln(\zeta)\Bigr]\biggr\}. \end{aligned} \tag{62}$$

The function $\mathcal{L}\mathrm{i}_2(x;y)$ is the continued dilogarithm

$$\mathcal{L}\mathrm{i}_2(x;y) = \mathrm{Li}_2(1-xy) + \ln(1-xy)\,[\ln(xy) - \ln(x) - \ln(y)], \tag{63}$$

with $\mathrm{Li}_2(x)$ the usual dilogarithm and x, y lying on the first Riemann sheet. The answer for the second infrared-finite scalar four-point function, D_{0124}, can be obtained from Eq. (62) by substituting $(p_1, k_1) \leftrightarrow (p_2, k_2)$.

3.2.2 Photon-pole part of the infrared-finite four-point function

As was explained in Sect. 3.1, the photon-pole part of a scalar function can be obtained from the full scalar function by subtracting the “particle”-pole contributions. According to Eq. (55), the “particle”-pole contributions in the lower half of the complex k_0-plane are given by

$$D_{0123}^{\text{part}} = \frac{1}{2\pi} \int_0^{\xi_1+\xi_2<1} \frac{d\xi_1\,d\xi_2}{A(\xi)}\,\theta[E(\xi)]\,\delta[p^2(\xi)]. \tag{64}$$

The integration area is defined by the θ-function for the energy and by the condition $\xi_1+\xi_2 < 1$. The allowed area of integration and the curve where the δ-function has a non-zero value are schematically shown in Fig. 4. The depicted situation represents the most general case for the kinematics we are interested in.

After the integration over the δ-function has been performed, one is left with a simple one-dimensional integration of logarithmic type. The final result is

$$D_{0123}^{\text{part}} = \frac{1}{8\pi M_W^2}\,\frac{1}{D_2-\zeta D_1}\Biggl[\ln(1-y_0x_s)-\ln(1-x_s/\zeta)\Biggr]. \qquad (65)$$

3.2.3 The virtual infrared-divergent four-point function

In this subsection we describe the calculation of the infrared-divergent scalar four-point function D_{0134}, which enters the non-factorizable corrections through the decomposition of the five-point function. Similar four-point functions may also appear in the initial–final state interactions, but, as was mentioned before, the interactions of this type vanish in the sum of virtual and real contributions. The four-point function

$$D_{0134} = \int \frac{d^4k}{(2\pi)^4}\,\frac{1}{[k^2-\lambda^2+io][D_1-2(p_1\cdot k)][-2(k_1\cdot k)+io][2(k_2\cdot k)+io]}. \qquad (66)$$

is infrared-divergent, because only one unstable particle is involved, which is not enough to regularize the divergence. Therefore we introduce a regulator mass λ for the photon in order to trace the cancellation of infrared divergences in virtual and real corrections. Again we can apply the Feynman-parameter technique as explained in Sect. 3.1. However, special care has to be taken with the photon mass λ. As usual we can introduce Feynman parameters according to

$$D_{0134} = 2\int_0^1 d^3\xi\,\delta\Bigl(1-\sum_{i=1}^{3}\xi_i\Bigr)\,I_{0134}(\xi), \qquad (67)$$

with

$$I_{0134}(\xi) = \int \frac{d^4k}{(2\pi)^4}\,\frac{1}{[k^2-\lambda^2+io][-k_0\,|E(\xi)|-\vec{k}\cdot\vec{p}(\xi)+A(\xi)+io]^3} \qquad (68)$$

and

$$A(\xi) = \xi_2\,D_1, \quad p^\mu(\xi) = -2\xi_1\,k_1^\mu - 2\xi_2\,p_1^\mu + 2\xi_3\,k_2^\mu. \qquad (69)$$

Again we can exploit the freedom to perform the variable transformation $k_0 \to -k_0$ in order to fix the sign of the energy component $E(\xi)$. After the integration over momentum space, the details of which can be found in App. A.3, we obtain

$$I_{0134}(\xi) = -\frac{i}{8\pi^2}\,\frac{\partial}{\partial p^2}\Biggl\{\frac{1}{\sqrt{A^2-\lambda^2p^2}}\ln\Biggl(\frac{A-\sqrt{A^2-\lambda^2p^2}}{A+\sqrt{A^2-\lambda^2p^2}}\Biggr)\Biggr\} \qquad (70)$$

with

$$\frac{p^2(\xi)}{4} = \xi_2^2M_W^2+\xi_1^2m_1^2+\xi_3^2m_2^2+\xi_1\xi_2M_W^2-\xi_1\xi_3s_{12}+\xi_2\xi_3(M_W^2-s_{211'}). \qquad (71)$$

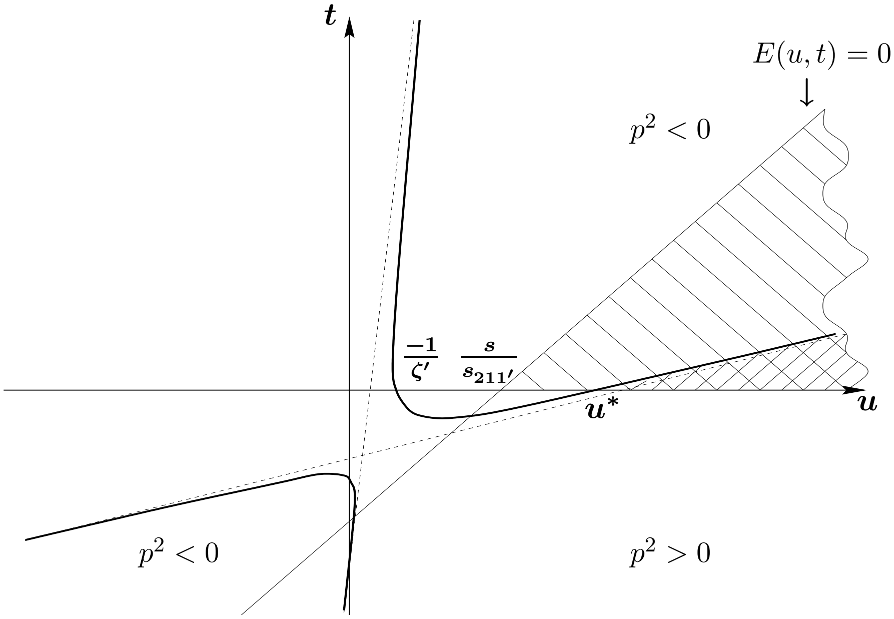

Figure 5: The area of integration in the (u, t)-plane for the calculation of the particle pole D_{0134}^{part}. The shaded region is the area of integration where $E(u, t) > 0$. The doubly-shaded region is the area of integration where $E(u, t) > 0$ and $p^2(u, t) > 0$. The thicker curves indicate the solutions of $p^2(u, t) = 0$, with $u^* = -\zeta' M_W^2/m_2^2$.

The masses of the final-state fermions, m_1 and m_2, are taken to be small in our approximation.

One is left with a twofold Feynman-parameter integration (see App. A.3), which results in

$$\begin{aligned} D_{0134} &= -\frac{i}{16\pi^2 s_{12}}\frac{1}{D_1}\bigg[\mathrm{Li}_2\Big(1+\frac{\zeta' M_W^2}{s_{12}}\Big) - 2\ln\Big(\frac{M_W\lambda}{-D_1}\Big)\ln\Big(\frac{m_1 m_2}{-s_{12}-io}\Big) \\ &\qquad + \frac{\pi^2}{3} + \ln^2\Big(\frac{M_W}{m_1}\Big) + \ln^2\Big(\frac{m_2}{\zeta' M_W}\Big)\bigg]. \end{aligned} \tag{72}$$

The answer for the second infrared-divergent scalar four-point function, D_{0234}, can be obtained from Eq. (72) by substituting $(p_1, k_1) \leftrightarrow (p_2, k_2)$.

3.2.4 Photon-pole part of the infrared-divergent four-point function

The procedure for calculating the photon-pole part D_{0134}^{γ} follows our general strategy, i.e. we calculate the corresponding "particle"-pole contributions and subtract them from the full virtual scalar function. The difference between this case and the one discussed in Sect. 3.2.2 lies in the fact that here both photon-pole and "particle"-pole contributions are infrared-divergent. So as to keep track of the cancellation of the infrared divergences, we again introduce a regulator mass λ for the photon.

In App. A.3 the following convenient representation for $I_{0134}(\xi)$ was derived in Eq. (155):

$$I_{0134}(\xi) = \frac{i}{16\pi^2|E(\xi)|}\int\limits_{-\infty}^{\infty}\frac{dz}{\Big[-|E(\xi)|\sqrt{z^2+\lambda^2}-|\vec{p}(\xi)|\,z+A(\xi)+io\Big]^2}. \tag{73}$$

From the general discussion in Sect. 3.1 we know that the photon-pole contribution to the four-point functions in the Feynman-parameter representation, $I^{\gamma}_{\mathrm{virt}}(\xi)$, can be obtained from the complete virtual function, $I_{\mathrm{virt}}(\xi)$, by a substitution $|E(\xi)| \to -E(\xi)$. Then the "particle"-pole contribution, $D^{\mathrm{part}}_{0134} = D_{0134} - D^{\gamma}_{0134}$, has the form

$$D^{\mathrm{part}}_{0134} = 2\int\limits_0^1 d^3\xi\,\delta\Big(1-\sum_{i=1}^{3}\xi_i\Big)\,I^{\mathrm{part}}_{0134}(\xi), \tag{74}$$

where

$$I^{\mathrm{part}}_{0134}(\xi) = -\frac{i\theta[E(\xi)]}{8\pi^2 E(\xi)}\,\frac{\partial}{\partial E(\xi)}\int\limits_{-\infty}^{+\infty}\frac{E(\xi)\,dz}{[E(\xi)]^2\,(z^2+\lambda^2)-(|\vec{p}(\xi)|\,z-A(\xi)-io)^2}. \tag{75}$$

By analysing the pole structure of the last expression, it is easy to realize that $I^{\mathrm{part}}_{0134}(\xi)$ is only non-vanishing for $p^2(\xi) \geq 0$. This results in a simple formula

$$I^{\mathrm{part}}_{0134}(\xi) = \frac{\theta[E(\xi)]}{4\pi}\,\frac{\partial}{\partial p^2(\xi)}\left\{\frac{\theta[p^2(\xi)]}{A(\xi)\sqrt{1-\frac{\lambda^2 p^2(\xi)}{[A(\xi)+io]^2}}}\right\}. \tag{76}$$

What is left is the integration over the space of Feynman parameters. In order to simplify the calculation it is advisable to make the change of variables $\xi_1 = t/(1{+}t{+}u)$ and $\xi_2 = 1/(1{+}t{+}u)$. The area of integration in the (u,t)-plane is shown schematically in Fig. 5. The final result is

$$D^{\mathrm{part}}_{0134} = \frac{1}{8\pi s_{12} D_1}\left[-\ln(-\zeta') + \ln\Big(\frac{D_1}{iM_W^2}\Big) - \ln\Big(\frac{\lambda}{m_2}\Big)\right]. \tag{77}$$

This is the same result as obtained in Sect. 4, where we will approach the various calculations in a significantly different way.

3.3 The Coulomb-like scalar three-point function

As was pointed out in Sect. 1.1, a gauge-invariant definition of the non-factorizable corrections requires the proper inclusion of a Coulomb-like contribution. In this subsection we calculate the associated scalar three-point function in the soft-photon approximation. This three-point function is infrared-finite, but ultraviolet-divergent. This divergence occurs as a result of the fact that we neglect the k^2 dependence of the propagators, following our general soft-photon strategy. Although the virtual and real Coulomb-like contributions to the cross-section are separately ultraviolet-divergent, the sum is finite.

The virtual Coulomb-like scalar three-point function C_{012} is defined as (see Fig. 2):

$$C_{012} = \int \frac{d^4k}{(2\pi)^4} \frac{1}{[k^2 + io][D_1 - 2(p_1 \cdot k)][D_2 + 2(p_2 \cdot k)]}. \tag{78}$$

Similar to the calculation of the scalar four-point functions, we introduce the Feynman parameters only for the propagators that are linear in k. We limit the area of integration over $\vec{k}$ by the condition $|\vec{k}| < \Lambda$, where $\Lambda \gg \Gamma_W$. After having performed the momentum integration, one is left with a one-dimensional integral over Feynman parameters:

$$\begin{aligned} C_{012} \;\; &= \;\; -\frac{i}{8\pi^2} \int\limits_0^1 d^2\xi\, \delta(1 - \xi_1 - \xi_2) \left[\frac{1}{|\vec{p}|\,(|E| - |\vec{p}|)} \ln\!\left(\frac{|E| - |\vec{p}| - A/\Lambda}{-A/\Lambda} \right) \right. \\ &\qquad \left. - \frac{1}{|\vec{p}|\,(|E| + |\vec{p}|)} \ln\!\left(\frac{|E| + |\vec{p}| - A/\Lambda}{-A/\Lambda} \right) \right], \end{aligned} \tag{79}$$

where $A(\xi) = \xi_1 D_1 + \xi_2 D_2$ and $p^\mu(\xi) = -2\xi_1 p_1^\mu + 2\xi_2 p_2^\mu$. The final integration over the Feynman parameters yields

$$\begin{aligned} C_{012} \;\; &= \;\; \frac{i}{16\pi^2 s\beta} \left\{ \mathcal{L}\mathrm{i}_2\!\left(y_0; \frac{1}{x_s} \right) + \mathcal{L}\mathrm{i}_2\!\left(\frac{1}{y_0}; \frac{1}{x_s} \right) - 2\,\mathrm{Li}_2\!\left(1 - \frac{1}{x_s} \right) + \frac{1}{2} \ln^2(y_0) \right. \\ &\qquad \left. + \ln(x_s) \left[\ln\!\left(\frac{-iD_1}{2M_W\Lambda} \right) + \ln\!\left(\frac{-iD_2}{2M_W\Lambda} \right) \right] - 2i\pi \ln\!\left(\frac{1 + x_s}{2} \right) \right\}. \end{aligned} \tag{80}$$

In a similar way one can calculate the particle-pole contribution C_{012}^{part}, which can be used to extract the photon-pole part $C_{012}^{\gamma} = C_{012} - C_{012}^{\mathrm{part}}$. The final answer for the particle-pole contribution reads

$$C_{012}^{\mathrm{part}} = \frac{1}{8\pi s\beta} \left\{ \ln(1 - x_s) + \ln(1 + x_s) - \ln(1 - y_0 x_s) - \ln\!\left(\frac{-iD_2}{M_W\Lambda} \right) \right\}. \tag{81}$$

Note that the real part of C_{012}^{part} does not contribute to the non-factorizable corrections. Therefore, the Λ dependence effectively drops out from the particle-pole contribution.

One may wonder how the non-factorizable contributions (2) and (3) to the cross-section compare with the Coulomb contribution as calculated in the literature. Our calculation is based on the assumption of being at least a few widths away from the threshold [the accuracy of this approximation is of $\mathcal{O}(\Gamma_W/\Delta E)$], whereas the Coulomb effect in the literature is valid in the non-relativistic region, where it approximates the cross-section with accuracy $\mathcal{O}(\beta)$. Therefore one could try to compare them in an overlapping region, where $\Gamma_W \ll \Delta E \ll M_W$. The Coulomb effect calculated in Ref. [8] consists of two parts. One contribution that is also present for on-shell W-bosons, and one that comes from the off-shellness. The former is related to factorizable corrections and the latter is related to non-factorizable corrections and vanishes upon integration over the virtualities[4]. In the overlap region ($\Gamma_W \ll \Delta E \ll M_W$) this off-shell term equals the $1/\beta$ part of our full expression.

---

[4] Only soft virtual photons contribute to both parts. For the on-shell (factorizable) part of the Coulomb

4 Direct momentum-integration method

In this section we present an alternative method of calculating the non-factorizable corrections, i.e. the so-called direct momentum-integration (DMI) method. As in Sects. 2 and 3, we use the soft-photon approximation and assume the charged final-state fermions to be massless, which is a good approximation for the process under consideration. In contrast to Sects. 2 and 3 we do not make any assumptions about the mass of the final-state neutrinos, because it does not simplify the calculation significantly. This gives us the opportunity to apply the results of this section to top-quark pair production. Following the approach of [9], we write the amplitudes corresponding to the diagrams shown in Fig. 1 in terms of virtual and real scalar four-/five-point functions. In contrast to the Feynman-parameter approach of Sect. 3, we do not introduce Feynman parameters, but perform instead a direct integration over momentum space [9]. The calculation can be considerably simplified by an appropriate choice of the frame.

First we calculate the infrared-finite virtual and real four-point functions. The calculation is close to the one presented in [9], but in contrast to [9] we make a clear separation between the virtual and real contributions. Our final result agrees with the one of [9], as well as with the one obtained in the MST in Sects. 3.2.1 and 3.2.2. Next we calculate the infrared-divergent virtual and real four-point functions. Again we perform a separation of the real and virtual contributions, and provide a careful treatment of the divergences. All this is needed in order to trace the cancellations of infrared and collinear divergences. We find complete agreement with our results obtained in Sects. 3.2.3 and 3.2.4. At the same time the structure of the divergences in our results appears to be significantly different from the one obtained by using the method of [9], even in the complete answer when virtual and real corrections are summed up. Although the infrared-divergent scalar four-point functions do not appear directly in the answer for the non-factorizable corrections, the observed difference with the method of [9] turns out to be indicative, because similar problems arise in the evaluation of the (infrared-divergent) five-point functions. Finally we calculate in the same way the virtual and real five-point functions. After summing up the virtual and real five-point functions, we find, in contrast to the result in [9], that all collinear divergences cancel exactly, even for cross-sections that are exclusive with respect to the virtualities of the W bosons.

In conclusion, the calculation presented in this section is an extension of the method of [9]. We provide a proper treatment of the infrared and collinear divergences, and make a clear separation of the virtual and real corrections. Because of this, the calculation becomes much more involved. We use the results obtained in this section as an independent check of the results of Sects. 2 and 3. Although the methods are completely different and the answer of this section is very complicated, a perfect numerical agreement between our two calculations is observed.

Before listing the various results, we first define the notation. For the calculations in the

---

effect photons with momenta $\omega \approx \beta^2 M_W$ and $|\vec{k}| \approx \beta M_W$ are important (hence k^2 can not be neglected in the propagators of the unstable particles). On the other hand, only photons with momenta $\omega \approx \Gamma_W$ and $|\vec{k}| \approx \Gamma_W/\beta$ give the leading contribution to the off-shell part of the Coulomb effect. Far from the threshold, where $\Gamma_W \ll \Delta E \ll M_W$, the two regions in the photon-momentum space are well separated. Because of this the effects are additive. Near threshold, where $\Gamma_W \approx \Delta E$, the two regions start to intersect.

DMI method we need to specify the momenta in the centre-of-mass frame of the initial state. Because of the soft-photon, double-pole ($D_{1,2} \ll M_W^2$) approximation, the four-momenta of the two intermediate W bosons are related in a simple way:

$$p_1^\mu = (E, \vec{p}) = E\,(1, \vec{v}\,) \quad \text{and} \quad p_2^\mu = (E, -\vec{p}) = E\,(1, -\vec{v}\,), \tag{82}$$

with $|\vec{v}| = \beta$ the (on-shell) velocity of the W bosons [see also Eq. (57)]. The other relevant momenta are

$$k_1^\mu = (E_1, \vec{k}_1) = E_1\,(1, \vec{v}_1) \quad \text{and} \quad k_2^\mu = (E_2, \vec{k}_2) = E_2\,(1, \vec{v}_2), \tag{83}$$

with $|\vec{v}_i| \equiv v_i = \sqrt{1 - m_i^2/E_i^2}$ for $(i = 1, 2)$. In addition we need the definition of some (polar) angles with respect to the direction of the W^+ boson: $\theta_i = \angle(\vec{v}, \vec{v}_i)$ and $x_i = \cos\theta_i$ for $(i = 1, 2)$. The difference of the azimuthal angles of $\vec{k}_1$ and $\vec{k}_2$ is given by ϕ_{12}. So, for $\sin\phi_{12} = 0$ the final-state three-momenta $\vec{k}_i$ and $\vec{k}_i'$ lie in one plane. In the plane spanned by $\vec{k}_1$ and $\vec{k}_2$ we define $\theta_{12} = \angle(\vec{v}_1, \vec{v}_2)$ and $x_{12} = \cos\theta_{12}$.

4.1 Non-factorizable infrared-finite corrections

In this subsection we briefly describe the calculation of the infrared-finite four-point functions in the DMI scheme, following Ref. [9]. The result agrees with the one presented in [9], so this subsection is merely presented for completeness. The contribution of the infrared-finite virtual four-point function D_{0124} to the non-factorizable matrix element is given by

$$M_{0124} = \bar{M}_B \, \frac{i}{D_1} \int \frac{d^4k}{(2\pi)^4} \, \frac{16\pi\alpha\,(p_1\cdot k_2)}{[k^2 + io][2(k\cdot k_2) + io][D_1 - 2(p_1\cdot k)][D_2 + 2(p_2\cdot k)]}, \tag{84}$$

where $M_B = \bar{M}_B/(D_1 D_2)$ is the Born matrix element of the process, involving the production of an intermediate W-boson pair and its subsequent decay. We start the calculation by decomposing the unstable W-boson propagators according to

$$\frac{1}{[D_1 - 2(p_1\cdot k)][D_2 + 2(p_2\cdot k)]} = \left[\frac{1}{D_1 - 2(p_1\cdot k)} + \frac{1}{D_2 + 2(p_2\cdot k)}\right] \frac{1}{D + 4\,\vec{p}\cdot\vec{k}}\,, \tag{85}$$

where $D = D_1 + D_2$. The first term has two particle poles: one in the lower and one in the upper half of the complex k_0-plane. We close the contour in the lower half-plane, resulting in one particle-pole and one photon-pole contribution. The second term has all its particle poles in the lower half-plane. By closing the integration contour in the upper half-plane, only one of the photon poles will contribute. Note that the above decomposition mixes photon- and particle-pole contributions. In order to avoid possible confusion with the pure photon- and particle-pole contributions, we will write $M_{0124}^{`\gamma'}$ and $M_{0124}^{`\text{part}'}$ if the decomposition is used.

4.1.1 Particle-pole residue

We first concentrate on the particle-pole residue contributing to the first term in Eq. (85). This particle pole is situated at $k_0 = \vec{v}_2\cdot\vec{k}$. The corresponding residue reads

$$M_{0124}^{\text{`part'}} = \bar{M}_B\,\frac{4\pi\alpha}{D_1}\,\frac{1-\beta x_2}{2E}\int\frac{d^3k}{(2\pi)^3[(\vec{v}_2\cdot\vec{k})^2-\vec{k}^2]}\,\frac{1}{[\frac{D}{2E}+2\vec{v}\cdot\vec{k}][\frac{D_1}{2E}-(\vec{v}_2-\vec{v})\cdot\vec{k}]}. \tag{86}$$

The propagators can be exponentiated by introducing an integration over "time":

$$M_{0124}^{\text{`part'}} = -\bar{M}_B\,\frac{4\pi\alpha}{D_1}\,\frac{1-\beta x_2}{2E}\int\limits_0^\infty d\tau\,d\tau_1\,e^{i[\frac{D}{2E}\tau+\frac{D_1}{2E}\tau_1]}\int\frac{d^3k}{(2\pi)^3}\,\frac{e^{i\vec{k}\cdot\vec{r}}}{(\vec{v}_2\cdot\vec{k})^2-\vec{k}^2}, \tag{87}$$

where

$$\vec{r} = 2\tau\,\vec{v} - \tau_1\,(\vec{v}_2-\vec{v}). \tag{88}$$

The integral is infrared-finite, so there is no need to introduce a non-zero photon mass as infrared regulator. The spatial integration can be recognized as a relativistic Coulomb potential of a moving particle:

$$\phi(r) = -4\pi\int\frac{d^3k}{(2\pi)^3}\,\frac{e^{i\vec{k}\cdot\vec{r}}}{(\vec{v}_2\cdot\vec{k})^2-\vec{k}^2} = \frac{1}{\sqrt{r_\parallel^2+r_\perp^2(1-v_2^2)}}. \tag{89}$$

Here $r_\parallel$ and $r_\perp$ are the absolute values of the components of $\vec{r}$ parallel and perpendicular to $\vec{v}_2$:

$$r_\parallel = 2\beta x_2\tau - (1-\beta x_2)\tau_1, \quad r_\perp = \beta(2\tau+\tau_1)\sin\theta_2. \tag{90}$$

Note that $1-v_2^2 = m_2^2/E_2^2$ is small, but finite.

To do the remaining integrations over τ and τ_1, we can make a change of variables according to $(\tau,\tau_1)\to(\xi,y)$, with $\tau=\xi y$, $\tau_1=\xi(1-y)$, and the Jacobian $|\frac{\partial(\tau,\tau_1)}{\partial(\xi,y)}| = \xi$. The area of integration changes from $\tau>0$ and $\tau_1>0$ to $\xi>0$ and $0<y<1$. After this change of variables, the quantities $r_\parallel$ and $r_\perp$ will be proportional to ξ, rendering the integration over ξ trivial. The last integral over y can be calculated in a straightforward way, yielding after some manipulations

$$\underline{x_2<0}\;:\quad M_{0124}^{\text{`part'}} = \bar{M}_B\,i\alpha\,\frac{1-\beta x_2}{D_1\eta(x_2)}\left[\ln\!\Big(\frac{D}{D_1}\Big)+\ln\!\Big(\frac{1-\beta x_2}{-2\beta x_2}\Big)\right], \tag{91}$$

$$\underline{x_2>0}\;:\quad M_{0124}^{\text{`part'}} = \bar{M}_B\,i\alpha\,\frac{1-\beta x_2}{D_1\eta(x_2)}\left[\ln\!\Big(\frac{\eta(x_2)}{D}\Big)+\ln\!\Big(\frac{\eta(x_2)}{D_1}\Big)+\ln\!\Big(\frac{2x_2(1-\beta x_2)}{\beta(1-x_2^2)}\Big)+\ln\!\Big(\frac{E_2^2}{m_2^2}\Big)\right], \tag{92}$$

where

$$\eta(x) = (1+x\beta)\,D_1 + (1-x\beta)\,D_2. \tag{93}$$

The result for $M_{0124}^{\text{`part'}}$ is not the same for $x_2<0$ and $x_2>0$. This is caused by the propagator decomposition (85). However, the complete result, with the photon-pole residue included, will be independent of the sign of x_2.

4.1.2 Photon-pole residues

Now we calculate the photon-pole residues. There are two such contributions, one in each of the terms in the decomposition (85). We will indicate these two contributions by $M_{0124}^{`\gamma',1}$ and $M_{0124}^{`\gamma',2}$, respectively. For $M_{0124}^{`\gamma',1}$ the contour is closed in the lower half of the complex k_0-plane. In that case the photon pole is situated at $k_0 = |\vec{k}| - io$, yielding

$$M_{0124}^{`\gamma',1} = \bar{M}_B \, \frac{\alpha}{2\pi} \, \frac{1-\beta x_2}{D_1} \int \frac{d^2\Omega_k}{2\pi} \, \frac{1}{\eta(x)\,(1-\vec{v}_2\!\cdot\!\vec{n}_k)} \left[\ln\!\left(\frac{2\beta x + io}{1-\beta x}\right) - \ln(D) + \ln(-D_1)\right]. \quad (94)$$

Here $\vec{n}_k$ stands for the unit vector in the $\vec{k}$ direction and Ω_k indicates the angular variables in spherical coordinates (with the polar axis defined along $\vec{p}$). For $M_{0124}^{`\gamma',2}$ the contour is closed in the upper half of the complex k_0-plane. The corresponding residue can be obtained from Eq. (94) by adding an overall minus sign and by substituting $\beta \to -\beta$ and $D_1 \leftrightarrow D_2$ inside the square brackets:

$$M_{0124}^{`\gamma',2} = -\bar{M}_B \, \frac{\alpha}{2\pi} \, \frac{1-\beta x_2}{D_1} \int \frac{d^2\Omega_k}{2\pi} \, \frac{1}{\eta(x)\,(1-\vec{v}_2\!\cdot\!\vec{n}_k)} \left[\ln\!\left(\frac{-2\beta x + io}{1+\beta x}\right) - \ln(D) + \ln(-D_2)\right]. \quad (95)$$

Next one can perform the integration over the azimuthal angle, with the help of the formula

$$\int_0^{2\pi} \frac{d\phi}{2\pi} \, \frac{1}{1-\vec{v}_i\!\cdot\!\vec{n}_k} = \frac{1}{|x-x_i|}. \quad (96)$$

This expression is a possible source of collinear divergences, which are regularized by introducing the small non-zero fermion masses. In terms of this regularization, $|x - x_i|$ is replaced by $\sqrt{(x-x_i)^2 + m_i^2(1-x_i^2)/E_i^2}$. The sum of the two photon-pole residues amounts to

$$M_{0124}^{`\gamma'} = \bar{M}_B \, \frac{\alpha}{2\pi} \, \frac{1-\beta x_2}{D_1} \int_{-1}^{1} \frac{dx}{\eta(x)\,|x-x_2|} \left\{\ln\!\left(\frac{1+\beta x}{1-\beta x}\right) + \ln\!\left(\frac{D_1}{D_2}\right) + i\pi[\theta(-x) - \theta(x)]\right\}. \quad (97)$$

The last integration gives rise to integrals of logarithmic and dilogarithmic type. Let us single out the answer for the θ-function-dependent terms:

$$M_{0124}^{`\gamma',\theta} = \bar{M}_B \, \frac{\alpha}{2\pi} \, \frac{1-\beta x_2}{D_1 \eta(x_2)} \, i\pi \left\{C_1[\theta(-x_2) - \theta(x_2)] + 2C_2\,\theta(x_2) + 2C_3\,\theta(-x_2)\right\}, \quad (98)$$

where

$$\begin{aligned} C_1 &= \ln\!\left(\frac{\eta(x_2)}{\eta(1)}\right) + \ln\!\left(\frac{\eta(x_2)}{\eta(-1)}\right) + \ln\!\left(\frac{4E_2^2}{m_2^2}\right), \quad C_2 = \ln\!\left(\frac{D}{\eta(-1)}\right) + \ln\!\left(\frac{1+x_2}{x_2}\right), \\ C_3 &= \ln\!\left(\frac{\eta(1)}{D}\right) + \ln\!\left(\frac{x_2}{x_2-1}\right). \end{aligned} \quad (99)$$

Separately, the particle-pole residue and the photon-pole residues depend on the sign of x_2. However, the sum of these terms does not. This dependence on x_2 at the intermediate stage of the calculation is a consequence of the decomposition of the unstable W-boson propagators.

The final answer for the contribution of the infrared-finite virtual four-point function D_{0124} to the non-factorizable matrix element is given by

$$
\begin{aligned}
M_{0124} \;=\; & \bar{M}_B\,\frac{\alpha}{2\pi}\,\frac{1-\beta x_2}{D_1\eta(x_2)}\biggl\{\Bigl[F_2(x_2|x_2)-F_2(-D_0|x_2)\Bigr]\ln\Bigl(\frac{D_1}{D_2}\Bigr) \\
& - F_1\Bigl(-D_0;\beta|x_2\Bigr)+F_1\Bigl(-D_0;-\beta|x_2\Bigr)+F_1\Bigl(x_2;\beta|x_2\Bigr)-F_1\Bigl(x_2;-\beta|x_2\Bigr) \\
& + i\pi\biggl[2\ln\Bigl(\frac{\eta(x_2)}{D_1}\Bigr)+\ln\Bigl(\frac{\eta(1)}{\eta(-1)}\Bigr)+2\ln\Bigl(\frac{1-\beta x_2}{\beta(1-x_2)}\Bigr)+\ln\Bigl(\frac{E_2^2}{m_2^2}\Bigr)\biggr]\biggr\},
\end{aligned}
\tag{100}
$$

where

$$
D_0=\frac{1}{\beta}\,\frac{D_1+D_2}{D_1-D_2}. \tag{101}
$$

The logarithmic and dilogarithmic functions $F_{1,2}$ can be found in App. C.1. The final answer for M_{0124} agrees with the answer presented in [9]. It is also in complete numerical and analytical agreement with the corresponding expression in Sect. 3, which was calculated with the help of the MST.

The contribution from the other infrared-finite virtual four-point function, D_{0123}, can be obtained from Eq. (100) by substituting $(p_1,k_1)\leftrightarrow(p_2,k_2)$.

4.1.3 The pure photon-pole part

As was already explained in Sect. 2.4, the photon-pole parts of the virtual scalar functions can be related to the corresponding bremsstrahlung interferences. To this end, one needs to calculate the pure photon-pole contribution to the matrix element, without performing the decomposition of the unstable W-boson propagators, since this decomposition mixes photon- and particle-pole contributions.

This calculation is pretty much the same as the one discussed in the previous subsection. We present only the answer:

$$
\begin{aligned}
M^{\gamma}_{0124} \;=\; & \bar{M}_B\,\frac{\alpha}{2\pi}\,\frac{1-\beta x_2}{D_1\eta(x_2)}\biggl\{\Bigl[\ln\Bigl(\frac{D_1}{D_2}\Bigr)+i\pi\Bigr]\Bigl[F_2(x_2|x_2)-F_2(-D_0|x_2)\Bigr]-F_1\Bigl(-D_0;\beta|x_2\Bigr) \\
& + F_1\Bigl(-D_0;-\beta|x_2\Bigr)+F_1\Bigl(x_2;\beta|x_2\Bigr)-F_1\Bigl(x_2;-\beta|x_2\Bigr)\biggr].
\end{aligned}
\tag{102}
$$

Note that the photon pole has been evaluated in the upper half of the complex k_0-plane. The reason for this lies in the fact that we have opted to perform the calculations in the most economic way. In this approach D^{γ}_{0124} is obtained from D^{γ}_{0123} by substituting $(p_1,k_1)\leftrightarrow(p_2,k_2)$, which automatically shifts the photon-pole from the lower to the upper half-plane (see Sect. 2.4).

4.2 The infrared-divergent scalar four-point function

In this subsection we present the calculation of the infrared-divergent virtual scalar four-point function D_{0134}. In the DMI method such functions are not needed for the calculation of the non-factorizable corrections. They arise only in the form of initial–final state interferences. Such corrections vanish when the corresponding bremsstrahlung interferences are taken into account, as was explained in Sect. 2.4. We perform the calculation mainly to study how one can handle infrared and collinear divergences in the DMI scheme and to provide an independent check of the results obtained in Sect. 3.

The infrared-divergent virtual scalar four-point function D_{0134} is defined as

$$D_{0134} = \int \frac{d^4k}{(2\pi)^4} \frac{1}{[k^2 - \lambda^2 + io][D_1 - 2(p_1 \cdot k)][-2(k_1 \cdot k) + io][2(k_2 \cdot k) + io]}. \tag{103}$$

We regularize the infrared divergences by introducing a regulator mass λ for the photon. There are also collinear divergences, which are regularized by the small non-zero fermion masses.

The pole structure of this integral is such that no propagator decomposition is required. There is one photon pole in each of the half-planes of the complex variable k_0. There are two particle poles in the upper half-plane, and only one in the lower half-plane. Therefore, we opt to close the integration contour in the lower half-plane, resulting in only two contributions to the scalar function: one photon-pole residue and one particle-pole residue.

4.2.1 Particle-pole contribution

One can proceed in the same way as in Sect. 4.1. We take the residue at the particle pole $k_0 = \vec{v}_2 \cdot \vec{k}$ and exponentiate the propagators by introducing an integration over "time":

$$D_{0134}^{\text{part}} = \frac{i}{8EE_1E_2} \int_0^\infty d\tau \, dt \, e^{i\tau \frac{D_1}{2E}} \int \frac{d^3k}{(2\pi)^3} \frac{e^{i\vec{r}\cdot\vec{k}}}{(\vec{k}\cdot\vec{v}_2)^2 - \vec{k}^2 - \lambda^2}, \tag{104}$$

where $\vec{r} = \tau\,(\vec{v} - \vec{v}_2) + t\,(\vec{v}_1 - \vec{v}_2)$. Again we can perform the integration over the momentum $\vec{k}$, which is similar to the λ-screened relativistic Coulomb potential of a moving particle. As the scalar function is infrared-divergent, one should keep the photon mass λ. The result of the integration is

$$\phi_\lambda(r) = -4\pi \int \frac{d^3k}{(2\pi)^3} \frac{e^{i\vec{r}\cdot\vec{k}}}{(\vec{k}\cdot\vec{v}_2)^2 - \vec{k}^2 - \lambda^2} = \frac{e^{-\frac{\lambda}{\sqrt{1-v_2^2}}\sqrt{r_\parallel^2 + r_\perp^2(1-v_2^2)}}}{\sqrt{r_\parallel^2 + r_\perp^2(1-v_2^2)}}. \tag{105}$$

Here both λ and $1 - v_i^2$ are small. We will consider the limit $\lambda \to 0$ and $v_i \to 1$, such that $\lambda \ll \sqrt{1 - v_i^2}$.

The particle-pole contribution now takes the form

$$D_{0134}^{\text{part}} = -\frac{i}{32\pi E E_1 E_2} \int\limits_0^\infty d\tau\, dt\, e^{i\tau \frac{D_1}{2E}} \, \frac{e^{-\frac{\lambda}{\sqrt{1-v_2^2}}\sqrt{r_\parallel^2 + r_\perp^2(1-v_2^2)}}}{\sqrt{r_\parallel^2 + r_\perp^2(1-v_2^2)}}, \tag{106}$$

where $r_\parallel^2 + r_\perp^2(1-v_2^2) = a + bt + ct^2$, with coefficients

$$\begin{aligned} a &= \tau^2(1-\beta x_2)^2 + \frac{m_2^2}{E_2^2}\,\tau^2\beta^2\sin^2\theta_2, \\ b &= 2\tau(1-x_{12})(1-\beta x_2) + 2\,\frac{m_2^2}{E_2^2}\,\tau\beta\sin\theta_2\sin\theta_{12}, \\ c &= (1-x_{12})^2 + \frac{m_2^2}{E_2^2}\sin^2\theta_{12}. \end{aligned} \tag{107}$$

The integral over t is logarithmically divergent in λ:

$$I_\lambda = \int\limits_0^\infty dt\, \frac{e^{-\frac{\lambda}{\sqrt{1-v_2^2}}\sqrt{a+bt+ct^2}}}{\sqrt{a+bt+ct^2}} \approx \frac{1}{\sqrt{c}}\left[-\mathbf{C} + \ln\!\Big(\frac{4\sqrt{c}\,m_2}{\lambda E_2\,(b+2\sqrt{ac}\,)}\Big)\right], \tag{108}$$

where $\mathbf{C}$ is the Euler constant.

The last integration over τ is relatively simple, yielding

$$D_{0134}^{\text{part}} = \frac{1}{8\pi s_{12}}\,\frac{1}{D_1}\left[\ln\!\Big(\frac{D_1}{iM_W^2}\Big) - \ln\!\Big(\frac{s_{211'}}{M_W^2} - 1\Big) - \ln\!\Big(\frac{\lambda}{m_2}\Big)\right]. \tag{109}$$

The invariants s_{12} and $s_{211'}$ are defined in Eq. (56).

4.2.2 Photon-pole contribution

Next the photon-pole residue at $k_0 = \omega = \sqrt{\vec{k}^2 + \lambda^2 - io}$ is determined:

$$D_{0134}^{\gamma} = -\frac{i}{16 E E_1 E_2}\int \frac{d^3k}{(2\pi)^3\omega}\,\frac{1}{(1-\beta x)[\omega - \frac{D_1}{2E(1-\beta x)}][\omega - |\vec{k}|\,(\vec{n}_k\!\cdot\!\vec{v}_1)][\omega - |\vec{k}|\,(\vec{n}_k\!\cdot\!\vec{v}_2)]}. \tag{110}$$

We want to keep the propagators $[\omega - |\vec{k}|\,(\vec{n}_k\cdot\vec{v}_i)]$ as they are, instead of writing them as $|\vec{k}|\,[1 - \vec{n}_k\cdot\vec{v}_i]$, as was done in Ref. [9]. Keeping the exact form of the propagators leads to double-logarithmic collinear divergences. If, instead, the simplified version were to be used, then the double-logarithmic terms would be lost, and one cannot be sure whether the single-logarithmic divergence and the finite part would be correct.

First we perform the integration over $|\vec{k}|$. The presence of λ in the light-fermion propagators complicates things considerably. The light-fermion propagators can be rewritten in the following way:

$$\frac{1}{[\omega - |\vec{k}|\,(\vec{n}_k\!\cdot\!\vec{v}_1)][\omega - |\vec{k}|\,(\vec{n}_k\!\cdot\!\vec{v}_2)]} = \frac{1}{|\vec{k}|\,(\vec{n}_k\!\cdot\!\vec{v}_1 - \vec{n}_k\!\cdot\!\vec{v}_2)}\left[\frac{1}{\omega - |\vec{k}|\,(\vec{n}_k\!\cdot\!\vec{v}_1)} - \frac{1}{\omega - |\vec{k}|\,(\vec{n}_k\!\cdot\!\vec{v}_2)}\right]. \tag{111}$$

After the integration over $|\vec{k}|$ the photon-pole contribution will be of the form

$$D^{\gamma}_{0134} = \frac{i}{16\pi^2 E_1 E_2 D_1}\,[I_0 + I_1 + I_2], \tag{112}$$

where

$$\begin{aligned} I_0 &= \int \frac{d^2\Omega_k}{4\pi}\,\frac{1}{[1-\vec{n}_k\!\cdot\!\vec{v}_1][1-\vec{n}_k\!\cdot\!\vec{v}_2]}\,\ln\!\Big(\frac{-D_1}{E\lambda(1-\beta x)}\Big), \\ I_1 &= \mathcal{P}\Big\{\int \frac{d^2\Omega_k}{4\pi}\,\frac{1}{[\vec{n}_k\!\cdot\!\vec{v}_1 - \vec{n}_k\!\cdot\!\vec{v}_2][1-(\vec{n}_k\!\cdot\!\vec{v}_1)^2]}\,\ln\!\Big(\frac{1-\vec{n}_k\!\cdot\!\vec{v}_1}{2}\Big)\Big\}. \end{aligned} \tag{113}$$

The expression for I_2 can be obtained from I_1 by the substitution $\vec{v}_1 \leftrightarrow \vec{v}_2$. The integral I_0 is similar to the one that shows up in the approach of [9]. It contains only single-logarithmic collinear divergences. The integrals $I_{1,2}$ are new and give rise to double-logarithmic terms. They are evaluated as a principal-value integral, since the singularity present in $1/[\vec{n}_k\!\cdot\!\vec{v}_1 - \vec{n}_k\!\cdot\!\vec{v}_2]$ is an artefact of the split-up (111) and disappears in the sum $I_1 + I_2$.

As a next step we integrate over the azimuthal angle ϕ. We obtain for the first integral

$$I_0 = \frac{1}{2(1-x_{12}^2)}\int_{-1}^{+1}\frac{dx}{(x-x_a)(x-x_b)}\left[\frac{J_1 - xK_1}{|x-x_1|} + \frac{J_2 - xK_2}{|x-x_2|}\right]\ln\!\Big(\frac{-D_1}{E\lambda(1-\beta x)}\Big), \tag{114}$$

with

$$\begin{aligned} x_{a,b} &= \frac{x_1 + x_2 \pm i\sin\theta_1\sin\theta_2\sin\phi_{12}}{1+x_{12}}, \\ J_1 &= 1 - x_{12} - x_1(x_1 - x_2), \quad K_1 = x_2 - x_1 x_{12}, \\ J_2 &= 1 - x_{12} - x_2(x_2 - x_1), \quad K_2 = x_1 - x_2 x_{12}. \end{aligned} \tag{115}$$

As indicated in Sect. 4.1, $|x - x_i|$ should be regularized by keeping the small non-zero fermion masses: $|x - x_i| \to \sqrt{(x-x_i)^2 + \mu_i^2}$, with $\mu_i^2 = m_i^2(1-x_i^2)/E_i^2$. Using the result for the principal-value integral given in App. C.2, we find for the second integral

$$I_1 = \frac{1}{4|\vec{v}_1 - \vec{v}_2|}\int_{x_+}^{1}\frac{dx}{\sqrt{x^2 - x_+^2}}\left[\frac{1}{1-v_1 x} + \frac{1}{1+v_1 x}\right]\ln\!\Big(\frac{1-v_1 x}{1+v_1 x}\Big), \tag{116}$$

where $x_\pm = \sqrt{(1 \pm x_{12})/2}\,$.

One is left with a one-dimensional integration over x. The integrals $I_{1,2}$ can be expressed in terms of the dilogarithmic functions $\mathcal{F}_1$ and $\mathcal{F}_2$, defined in App. C.3:

$$I_{1,2} = \frac{1}{8x_-}\,[\mathcal{F}_1(x_+; v_{1,2}) + \mathcal{F}_2(x_+)]. \tag{117}$$

The answer for the integral I_0 is

$$\begin{aligned} I_0 &= \frac{1}{1-x_{12}}\ln\Big(\frac{E\lambda\beta}{-D_1}\Big)\ln\Big(\frac{m_1m_2}{s_{12}}\Big) - \sum_{i=1}^{2}\frac{x_i-x_a}{4(1-x_{12})}\,\mathcal{K}(-x_a;\frac{1}{\beta}|x_i;\mu_i^2) \\ &\quad - \sum_{i=1}^{2}\frac{x_i-x_b}{4(1-x_{12})}\,\mathcal{K}(-x_b;\frac{1}{\beta}|x_i;\mu_i^2), \qquad (118) \end{aligned}$$

where the function $\mathcal{K}$ is introduced in App. C.3.

The complete expression for the infrared-divergent scalar four-point function is obtained as the sum of the particle-pole and photon-pole contributions. When comparing all the above results with the ones obtained in Sects. 3.2.3 and 3.2.4, complete numerical agreement is found for both virtual and real four-point functions, including collinear and infrared divergences.

4.3 Non-factorizable corrections from the five-point functions

In this subsection we describe the calculation of the scalar five-point functions using the DMI method. The contribution of the virtual five-point function to the non-factorizable matrix element is given by

$$M = i\bar{M}_B\int\frac{d^4k}{(2\pi)^4}\,\frac{16\pi\alpha\,(k_1\cdot k_2)}{[k^2-\lambda^2+io][-2(k\cdot k_1)+io][2(k\cdot k_2)+io][D_1-2(k\cdot p_1)][D_2+2(k\cdot p_2)]}. \qquad (119)$$

In analogy to Sect. 4.1, one can perform a decomposition of the unstable W-boson propagators

$$\frac{1}{[D_1-2(p_1\cdot k)][D_2+2(p_2\cdot k)]} = \Big[\frac{1}{D_1-2(p_1\cdot k)}+\frac{1}{D_2+2(p_2\cdot k)}\Big]\frac{1}{D+4\vec{p}\cdot\vec{k}}\,. \qquad (120)$$

In this way the matrix element splits into two terms. If the integration contour in the complex k_0-plane is chosen properly, each term involves one photon-pole contribution and one particle-pole contribution.

4.3.1 Particle-pole residues

We first calculate the particle-pole residue that contributes to the first term in Eq. (120). We proceed in the usual way, by taking the residue at $k_0=\vec{v}_2\cdot\vec{k}$ and subsequently exponentiating the propagators. In this case this procedure requires three integrations:

$$M_2^{\text{`part'}} = \bar{M}_B\,\frac{i\pi\alpha}{2}\,\frac{1-x_{12}}{E^2}\int\limits_0^\infty dt\,d\tau\,d\tau_1\,e^{i\left[\frac{D}{4E}\tau+\frac{D_1}{2E}\tau_1\right]}\int\frac{d^3k}{(2\pi)^3}\,\frac{e^{i\vec{r}_2\cdot\vec{k}}}{(\vec{k}\cdot\vec{v}_2)^2-\vec{k}^2-\lambda^2}, \qquad (121)$$

where $\vec{r}_2=\tau\,\vec{v}+\tau_1\,(\vec{v}-\vec{v}_2)+t\,(\vec{v}_1-\vec{v}_2)$. The integral over d^3k is the same as the one evaluated for the calculation of the infrared-divergent four-point function [see Eq. (105)]. Again, a non-zero photon mass λ is needed for the regularization of the infrared divergences. The particle-pole residue now amounts to

$$M_2^{\text{`part'}} = -\bar{M}_B \, \frac{i\alpha}{8} \, \frac{1-x_{12}}{E^2} \int\limits_0^\infty dt\, d\tau\, d\tau_1 \, e^{i\left[\frac{D}{4E}\tau + \frac{D_1}{2E}\tau_1\right]} \, \frac{e^{-\frac{\lambda}{\sqrt{1-v_2^2}}\sqrt{r_\parallel^2 + r_\perp^2(1-v_2^2)}}}{\sqrt{r_\parallel^2 + r_\perp^2(1-v_2^2)}}, \tag{122}$$

where $r_\parallel^2 + r_\perp^2(1-v_2^2) = a + bt + ct^2$, with coefficients

$$\begin{aligned}
a &= [\tau\beta x_2 - \tau_1(1-\beta x_2)]^2 + \frac{m_2^2}{E_2^2}\,(\tau+\tau_1)^2\beta^2\sin^2\theta_2, \\
b &= -2(1-x_{12})[\tau\beta x_2 - \tau_1(1-\beta x_2)] + 2\,\frac{m_2^2}{E_2^2}\,\beta(\tau+\tau_1)\sin\theta_{12}\sin\theta_2, \\
c &= (1-x_{12})^2 + \frac{m_2^2}{E_2^2}\sin^2\theta_{12}.
\end{aligned} \tag{123}$$

Following Sect. 4.2, first the integration over t is performed, yielding the logarithmically-divergent result

$$M_2^{\text{`part'}} = -\bar{M}_B \, \frac{i\alpha}{8E^2} \int\limits_0^\infty d\tau\, d\tau_1 \, e^{i\left[\frac{D}{4E}\tau + \frac{D_1}{2E}\tau_1\right]} \left[-\mathbf{C} + \ln\!\left(\frac{4\sqrt{c}\, m_2}{\lambda E_2\,(b + 2\sqrt{ac}\,)} \right) \right], \tag{124}$$

To linearize $b + 2\sqrt{ac}$ with respect to one of the integration variables, one should make a change of variables according to $(\tau, \tau_1) \to (\xi, y)$, with $\tau = \xi y$, $\tau_1 = \xi(1-y)$. In this way, the integration over ξ can be trivially performed:

$$M_2^{\text{`part'}} = \bar{M}_B \, \frac{i\alpha}{8E^2} \int\limits_0^1 \frac{dy}{\left[\frac{D}{4E}y + \frac{D_1}{2E}(1-y)\right]^2} \left\{ -1 + \ln\!\left(\frac{4m_2(1-x_{12})}{\lambda E_2\,(b' + 2\sqrt{a'c'})} \right) + \ln\!\left(\frac{Dy + 2D_1(1-y)}{4iE} \right) \right\}, \tag{125}$$

where the coefficients a', b', and c' follow from the coefficients a, b, and c, by substituting $\tau \to y$ and $\tau_1 \to (1-y)$.

The last integration is technically quite involved, but only gives rise to logarithms. Note that one should carefully analyse the infrared and collinear divergences, present in this integral. The final answer is formally different for $x_2 < 0$ and $x_2 > 0$. This is the same phenomenon as observed in Sect. 4.1, which can be attributed to the decomposition of the W-boson propagators. The result for the photon-pole residue will compensate this dual behaviour, leading to a combined result that is analytically the same for both $x_2 < 0$ and $x_2 > 0$. In a similar way the second particle-pole residue, corresponding to the second term in Eq. (120), will formally depend on the sign of x_1.

We will not bore the reader with all the different cases and merely present the answer for the case $x_1 > 0$, $x_2 < 0$. Taking into account both particle-pole residues, the final answer reads

$\underline{x_1 > 0,\ x_2 < 0}$:

$$
\begin{aligned}
M^{\text{`part'}} \;=\; & -\bar{M}_B\,\frac{i\alpha}{2}\left\{\frac{2}{D_1 D}\ln\Bigl(\frac{2\lambda E}{M_W^2}\Bigr)+\frac{2}{D_1 D}\ln\Bigl(\frac{E_2}{m_2}\Bigr)+\frac{2}{D_2 D}\ln\Bigl(\frac{D}{iM_W^2}\Bigr)-\frac{2}{D_1 D_2}\ln\Bigl(\frac{D_1}{iM_W^2}\Bigr)\right.\\
& \left.+\frac{2(1-\beta x_2)}{D_1\eta(x_2)}\ln(1-\beta x_2)-\frac{2(1+\beta x_2)}{D_2\eta(x_2)}\ln\Bigl(\frac{D}{D_1}\Bigr)+\frac{4\beta x_2}{D\eta(x_2)}\ln(-2\beta x_2)\right\}\\
& -\bar{M}_B\,\frac{i\alpha}{2}\Bigl\{x_2\to x_1,\ m_2\to m_1,\ E_2\to E_1,\ D_1\leftrightarrow D_2,\ \beta\to-\beta\Bigr\}. \qquad (126)
\end{aligned}
$$

Note that the terms $\ln(\frac{E_2}{m_2})$ and $\ln(\frac{E_1}{m_1})$ cause the difference with the results presented in Ref. [9].

4.3.2 Photon-pole residues

Next we determine the photon-pole residues. Each of the terms in the propagator decomposition (120) gives rise to one photon-pole residue, situated at $k_0=\omega=\pm\sqrt{\vec{k}^2+\lambda^2-io}$. In the same way as in Sect. 4.2, the light-fermion propagators occurring in the photon-pole residues can be rewritten according to Eq. (111). Again we introduce spherical coordinates, with the polar axis defined along $\vec{p}$. For the integration over $|\vec{k}|$ we keep the λ dependence of ω in order to get the correct divergences. The combined result of all photon-pole residues is given by

$$
M^{\text{`}\gamma\text{'}} = -\bar{M}_B\,\frac{\alpha}{\pi}\,(1-x_{12})\int\frac{d^2\Omega_k}{4\pi}\left\{\frac{\Psi(D_1,D_2,x)}{(1-\alpha_1)(1-\alpha_2)}+\frac{1}{D_1D_2}\Bigl[\Phi(\alpha_1,\alpha_2)+\Phi(\alpha_2,\alpha_1)\Bigr]\right\}, \qquad (127)
$$

with

$$
\begin{aligned}
\Psi(D_1,D_2,x) &= \Psi_0+\Psi_{12}+\Psi_\theta,\\
\Psi_0 &= -\frac{1}{D_1D_2}\Bigl[\ln\Bigl(\frac{\lambda E}{M_W^2}\Bigr)+i\pi\Bigr],\\
\Psi_{12} &= \frac{1-\beta x}{D_1\eta(x)}\,\ln\Bigl(\frac{D_1}{M_W^2\,(1-\beta x)}\Bigr)+\frac{1+\beta x}{D_2\eta(x)}\,\ln\Bigl(\frac{D_2}{M_W^2\,(1+\beta x)}\Bigr),\\
\Psi_\theta &= \frac{2\beta x}{D\eta(x)}\,i\pi\,[\theta(\beta x)-\theta(-\beta x)],\\
\Phi(\alpha_1,\alpha_2) &= \frac{1}{(\alpha_1-\alpha_2)(1-\alpha_1^2)}\,\ln\Bigl(\frac{1-\alpha_1}{2}\Bigr), \qquad (128)
\end{aligned}
$$

and $\alpha_i=(\vec{n}_k\cdot\vec{v}_i)$ for $(i=1,2)$.

The Ψ-term in Eq. (127) also emerges in the calculations presented in [9], up to the divergent term $\ln(\lambda E)$. This Ψ-term contains infrared divergences and logarithmic collinear divergences. The other two terms in Eq. (127) are of a type that was already encountered in Sect. 4.2. They will give rise to double-logarithmic collinear divergences

As in Sect. 4.2, we proceed by performing the azimuthal integration. The remaining integration over $x=\cos\theta$ gives logarithms and dilogarithms. Most of the ingredients of this final step in the calculation have already been discussed in the previous subsections. Therefore we only give the answer. First we do so for the Ψ_θ-terms. As was observed for the particle-pole residues, the results depend on the sign of $x_{1,2}$. Adopting the same sign choice as in Eq. (126), we obtain

$\underline{x_1 > 0,\ x_2 < 0}$:

$$\begin{aligned} M_\theta^{\text{‘}\gamma\text{’}} &= \bar{M}_B\,\frac{\alpha}{2\pi}\,i\pi\,\frac{1}{D}\biggl\{\mathcal{R}_{\eta,2}\Bigl[\ln\Bigl(\frac{\eta(-1)}{\eta(1)}\Bigr) - 2\ln\Bigl(\frac{\eta(x_2)}{D}\Bigr)\Bigr] + \mathcal{R}_2\Bigl[\ln\Bigl(\frac{4E_2^2}{m_2^2}\Bigr) + 2\ln\Bigl(\frac{-x_2}{1-x_2}\Bigr)\Bigr] \\ &\qquad\qquad + \sum_{j=a,b}\mathcal{R}_j\Bigl[\ln\Bigl(\frac{-1-x_j}{1-x_j}\Bigr) - 2\ln\Bigl(\frac{x_2-x_j}{-x_j}\Bigr)\Bigr]\biggr\} \\ &\quad + \bar{M}_B\,\frac{\alpha}{2\pi}\,i\pi\,\frac{1}{D}\biggl\{\mathcal{R}_{\eta,1}\Bigl[\ln\Bigl(\frac{\eta(-1)}{\eta(1)}\Bigr) + 2\ln\Bigl(\frac{\eta(x_1)}{D}\Bigr)\Bigr] - \mathcal{R}_1\Bigl[\ln\Bigl(\frac{4E_1^2}{m_1^2}\Bigr) + 2\ln\Bigl(\frac{x_1}{1+x_1}\Bigr)\Bigr] \\ &\qquad\qquad + \sum_{j=a,b}\mathcal{R}_j\Bigl[\ln\Bigl(\frac{-1-x_j}{1-x_j}\Bigr) + 2\ln\Bigl(\frac{x_1-x_j}{-x_j}\Bigr)\Bigr]\biggr\}. \end{aligned} \tag{129}$$

The coefficients $\mathcal{R}$ are given by $(i = 1, 2)$

$$\mathcal{R}_{\eta,i} = 2\beta D\,\frac{K_i\,D + \beta J_i\,(D_1 - D_2)}{(1 + x_{12})\,\eta(x_a)\,\eta(x_b)\,\eta(x_i)}, \quad \mathcal{R}_i = \frac{2\beta x_i}{\eta(x_i)} \quad \text{and} \quad \mathcal{R}_{a,b} = -\frac{\beta x_{a,b}}{\eta(x_{a,b})}. \tag{130}$$

As in Sect. 4.1, only the sum of the particle-pole residues and $M_\theta^{\text{‘}\gamma\text{’}}$ is independent of the sign of $x_{1,2}$.

The evaluation of the remaining terms in Eq. (127) is straightforward. The answers for the Ψ_0 - and Φ-terms are given by

$$M_0^{\text{‘}\gamma\text{’}} = -\bar{M}_B\,\frac{\alpha}{\pi}\,\frac{1}{D_1D_2}\,\ln\Bigl(\frac{m_1m_2}{s_{12}}\Bigr)\Bigl[\ln\Bigl(\frac{\lambda E}{M_W^2}\Bigr) + i\pi\Bigr], \tag{131}$$

$$M_\phi^{\text{‘}\gamma\text{’}} = -\bar{M}_B\,\frac{\alpha}{2\pi}\,\frac{1 - x_{12}}{D_1D_2}\,\frac{1}{4x_-}\,[\mathcal{F}_1(x_+;v_2) + \mathcal{F}_1(x_+;v_1) + 2\,\mathcal{F}_2(x_+)]. \tag{132}$$

The functions $\mathcal{F}_1$ and $\mathcal{F}_2$ can be found in App. C.3.

Finally, the answer for the Ψ_{12} -term reads

$$M_{12}^{\text{‘}\gamma\text{’}} = M_1^{\text{‘}\gamma\text{’}} + M_2^{\text{‘}\gamma\text{’}}, \tag{133}$$

with

$$\begin{aligned} M_2^{\text{‘}\gamma\text{’}} &= -\,\bar{M}_B\,\frac{\alpha}{2\pi}\biggl\{\frac{1-\beta x_2}{D_1\eta(x_2)}\Bigl[\ln\Bigl(\frac{4E_2^2}{m_2^2}\Bigr)\ln\Bigl(\frac{D_1}{M_W^2}\Bigr) - F_1(x_2;-\beta|x_2)\Bigr] \\ &\qquad - \sum_{i=a,b}\frac{1-\beta x_i}{2D_1\eta(x_i)}\Bigl[\ln\Bigl(\frac{D_1}{M_W^2}\Bigr)F_2(x_i|x_2) - F_1(x_i;-\beta|x_2)\Bigr] \\ &\qquad - \frac{R_{\eta,2}}{D}\Bigl[\ln\Bigl(\frac{D_1}{M_W^2}\Bigr)F_2(-D_0|x_2) - F_1(-D_0;-\beta|x_2)\Bigr]\biggr\} \\ &\quad -\,\bar{M}_B\,\frac{\alpha}{2\pi}\Bigl\{D_1 \leftrightarrow D_2,\ \beta \to -\beta\Bigr\}. \end{aligned} \tag{134}$$

Here D_0 is defined in Eq. (101) and the functions F_1 and F_2 are given in App. C.1. Note that the coefficient $R_{\eta,2}$ depends on β. The contribution $M_1^{\text{`}\gamma\text{'}}$ can be obtained by substituting $(E_2,\, m_2,\, x_2) \leftrightarrow (E_1,\, m_1,\, x_1)$ in Eq. (134).

The final answer for the contribution of the virtual five-point function to the non-factorizable matrix element can be obtained as

$$M = M^{\text{`part'}} + M_\theta^{\text{`}\gamma\text{'}} + M_0^{\text{`}\gamma\text{'}} + M_{12}^{\text{`}\gamma\text{'}} + M_\phi^{\text{`}\gamma\text{'}}, \tag{135}$$

with the various contributions given by Eqs. (126) and (129)–(134). This answer was compared numerically with the corresponding MST-expression in Sect. 2, which was derived by means of a decomposition of the five-point function into a sum of four-point functions. A complete numerical agreement was observed.

4.3.3 Pure photon-pole part

In order to calculate the real-photon radiative interference corresponding to the five-point function, one has to determine the photon-pole residue in the lower half-plane, without performing the propagator decomposition. The calculation is more or less the same as the one discussed in the previous subsection.

The answer can be written as

$$M^\gamma = M_0^\gamma + M_1^\gamma + M_2^\gamma + M_\phi^{\text{`}\gamma\text{'}}. \tag{136}$$

Note that the $M_\phi^{\text{`}\gamma\text{'}}$ contribution is the same as before [see Eq. (132)]. The other contributions are changed slightly:

$$M_0^\gamma = -\bar{M}_B\,\frac{\alpha}{\pi}\,\frac{1}{D_1 D_2}\,\ln\!\Big(\frac{m_1 m_2}{s_{12}}\Big)\,\ln\!\Big(\frac{\lambda E}{M_W^2}\Big), \tag{137}$$

and

$$\begin{aligned} M_2^\gamma \;=\; & M_2^{\text{`}\gamma\text{'}} + \bar{M}_B\,\frac{\alpha}{2\pi}\,i\pi\,\Bigg\{\frac{1-\beta x_2}{D_1\eta(x_2)}\,\ln\!\Big(\frac{4E_2^2}{m_2^2}\Big) - \sum_{i=a,b}\frac{1-\beta x_i}{2D_1\eta(x_i)}\,F_2(x_i|x_2) \\ & - \frac{R_{\eta,2}}{D}\,F_2(-D_0|x_2)\Bigg\}. \end{aligned} \tag{138}$$

The contribution M_1^γ can be obtained by substituting $(E_2,\, m_2,\, x_2) \leftrightarrow (E_1,\, m_1,\, x_1)$.

5 Complete results

Up to now we have focused on the case of purely leptonic final states. For the purely hadronic ones there are many more diagrams, as the photon can interact with all four final-state fermions.

In order to make efficient use of the results presented in the previous sections, we first introduce some short-hand notations based on the results for the purely leptonic (LL) final states. These short-hand notations involve the summation of virtual and real corrections to the differential cross-section. For instance, the virtual corrections originating from the first diagram of Fig. 1 can be combined with the corresponding real-photon correction into the contribution $d\sigma^{(4)}_{LL}(k_1;k_1'|p_2)$. In a similar way, virtual and real five-point corrections can be combined into $d\sigma^{(5)}_{LL}(k_1;k_1'|k_2;k_2')$. The gauge-restoring "Coulomb" contribution will be indicated by $d\sigma^{\mathrm{C}}(p_1|p_2)$. In terms of this notation the non-factorizable differential cross-section for purely leptonic final states becomes

$$d\sigma_{LL}(k_1;k_1'|k_2;k_2') = d\sigma^{(4)}_{LL}(k_1;k_1'|p_2) + d\sigma^{(4)}_{LL}(k_2;k_2'|p_1) + d\sigma^{(5)}_{LL}(k_1;k_1'|k_2;k_2') + d\sigma^{\mathrm{C}}(p_1|p_2). \quad (139)$$

Analogously the non-factorizable differential cross-section for a purely hadronic final state (HH) can be written in the following way

$$\begin{aligned} d\sigma_{HH}(k_1;k_1'|k_2;k_2') = 3\times 3\Big[&\frac{1}{3}\,d\sigma^{(4)}_{LL}(k_1;k_1'|p_2) + \frac{2}{3}\,d\sigma^{(4)}_{LL}(k_1';k_1|p_2) + \frac{1}{3}\,d\sigma^{(4)}_{LL}(k_2;k_2'|p_1) \\ &+ \frac{2}{3}\,d\sigma^{(4)}_{LL}(k_2';k_2|p_1) + \frac{1}{3}\cdot\frac{1}{3}\,d\sigma^{(5)}_{LL}(k_1;k_1'|k_2;k_2') + \frac{2}{3}\cdot\frac{1}{3}\,d\sigma^{(5)}_{LL}(k_1';k_1|k_2;k_2') \\ &+ \frac{1}{3}\cdot\frac{2}{3}\,d\sigma^{(5)}_{LL}(k_1;k_1'|k_2';k_2) + \frac{2}{3}\cdot\frac{2}{3}\,d\sigma^{(5)}_{LL}(k_1';k_1|k_2';k_2) + d\sigma^{\mathrm{C}}(p_1|p_2)\Big]. \end{aligned} \quad (140)$$

In order to keep the notation as uniform as possible, the momenta of the final-state quarks are defined along the lines of the purely leptonic case with k_i (k_i') corresponding to down- (up-) type quarks. If one would like to take into account quark-mixing effects, it suffices to add the appropriate squared quark-mixing matrix elements ($|V_{ij}|^2$) to the overall factor. Note that top quarks do not contribute to the double-pole residues, since the on-shell decay $W\to tb$ is not allowed. Therefore the approximation of massless final-state fermions is still justified.

For a semileptonic final state (say HL), when the W^+ decays hadronically and the W^- leptonically, one can write

$$\begin{aligned} d\sigma_{HL}(k_1;k_1'|k_2;k_2') = 3\Big[&\frac{1}{3}\,d\sigma^{(4)}_{LL}(k_1;k_1'|p_2) + \frac{2}{3}\,d\sigma^{(4)}_{LL}(k_1';k_1|p_2) + d\sigma^{(4)}_{LL}(k_2;k_2'|p_1) \\ &+ \frac{1}{3}\,d\sigma^{(5)}_{LL}(k_1;k_1'|k_2;k_2') + \frac{2}{3}\,d\sigma^{(5)}_{LL}(k_1';k_1|k_2;k_2') + d\sigma^{\mathrm{C}}(p_1|p_2)\Big]. \end{aligned} \quad (141)$$

Upon integration over the decay angles, the functions $d\sigma^{(5)}_{LL}$ and $d\sigma^{(4)}_{LL}$ become symmetric under $k_i \leftrightarrow k_i'$. As a result, expressions (140) and (141) take on the form of (139) multiplied by the colour factors 9 and 3, respectively. These are precisely the colour factors that also arise in the Born cross-section. Therefore, after integration over the decay angles, the relative non-factorizable correction is the same for all final states. This universality property holds for all situations that exhibit the $k_i \leftrightarrow k_i'$ symmetry. This means that there is only sensitivity to the charges of the decaying particles.

At this point one may wonder how non-factorizable corrections affect Z-pair-mediated and ZH-mediated four-fermion final states. In those cases, only five-point functions contribute, of which there are four contributions, as in Eq. (140). However, in contrast to Eq. (140), the charge factors are pair-wise opposite, such that integration over the decay angles leads to a vanishing result. Thus $\mathcal{O}(\alpha)$ non-factorizable corrections to invariant-mass distributions in Z-pair-mediated or ZH-mediated four-fermion processes vanish. This can be viewed as a consequence of the zero charges of the decaying particles.

6 Conclusions

In this paper we studied two methods to evaluate non-factorizable QED corrections in the double-pole, soft-photon approximation. We derived results for W-pair production, which are valid a few widths above threshold.

One technique (DMI) is an extension of that of Ref. [9] in the sense that the virtual and real photonic corrections are clearly separated and also regularized by a photon mass λ and charged-fermion masses m_1 and m_2. The resulting formulae are rather complicated and are different from those of [9].

The second method (MST) extends the standard technique in the sense that five-point bremsstrahlung interference terms are decomposed into four-point terms and that the soft-photon approximation is used from the start in the evaluation of real and virtual n-point functions. The results obtained with this method are much simpler than the DMI ones, but the two are in complete numerical agreement.

The MST can be easily generalized to more involved final states by a straightforward extension of the decomposition of five-point functions to the decomposition of n-point functions.

The methods and most of the actual formulae in this paper can also be applied to ZZ, ZH production and to top-quark pair production with subsequent Wb decays. In the latter case the top-quark, W and b take the rôle of W, ν and ℓ, the gluon that of the photon. In that case the DMI formulae are directly applicable since no assumption on the neutrino mass was made. The MST formulae would need a small modification.

A Feynman-parameter integrals

A.1 The on-shell four-point function

In this appendix we use Ref. [12] to present a compact expression for the on-shell four-point function D_{1234}, which appears in the decomposition of the virtual five-point function in Sect. 2.3. The result for D^R_{1234} can be obtained from D_{1234} by the substitutions $p_1 \to -p_1$ and $k_1 \to -k_1$. The results of [13] provide an independent check on the formula presented here.

As was mentioned before, the four-point function D_{1234} has to be calculated without soft-photon approximation and in the on-shell limit. The resulting function, defined as

$$D_{1234} = \int \frac{d^4k}{(2\pi)^4} \frac{1}{[(k-p_1)^2 - M_W^2][(k+p_2)^2 - M_W^2][(k-k_1)^2 - m_1^2][(k+k_2)^2 - m_2^2]}, \tag{142}$$

does not contain any divergences. Upon neglecting the fermion masses m_1 and m_2, the answer reads

$$M_W^2 a(x_1 - x_2) D_{1234} = \frac{i}{16\pi^2} \sum_{k=1}^{2} (-1)^k \Big\{ \mathcal{L}\mathrm{i}_2\Big(r_{14}; -x_k\Big) + \mathcal{L}\mathrm{i}_2\Big(\frac{1}{r_{14}}; -x_k\Big)$$
$$- \mathcal{L}\mathrm{i}_2\Big(-\frac{2(p_2 \cdot k_1)}{M_W^2} - io; -x_k\Big) - \mathcal{L}\mathrm{i}_2\Big(-\frac{M_W^2}{2(p_1 \cdot k_2)} + io; -x_k\Big) + \ln(-x_k) \ln\Big[\frac{(p_1 \cdot k_2)}{(k_1 \cdot k_2)}\Big]\Big\}, \tag{143}$$

where r_{14} is a solution of the equation

$$r_{14} + \frac{1}{r_{14}} = -\frac{s - 2M_W^2}{M_W^2} - io. \tag{144}$$

The quantities $x_{1,2}$ are the solutions of the equation

$$ax^2 + bx + c + ido = 0, \tag{145}$$

with coefficients

$$a = 2(k_1 \cdot k_2) - 2(p_2 \cdot k_1), \quad c = 2(k_1 \cdot k_2) - 2(p_1 \cdot k_2),$$
$$b = M_W^2 + \frac{4(p_1 \cdot k_2)(p_2 \cdot k_1)}{M_W^2} - \frac{4(p_1 \cdot p_2)(k_1 \cdot k_2)}{M_W^2}, \quad d = -2(k_1 \cdot k_2). \tag{146}$$

A.2 The infrared-finite four-point function

In this appendix we briefly describe some of the details of the Feynman-parameter integral belonging to D_{0123} (see Sect. 3.2.1). The integral to be evaluated is given by Eq. (59). In the notation adopted in Sect. 3 this integral reads

$$D_{0123} = -\frac{i}{4\pi^2 D_2} \int_0^1 d\xi_1 \int_0^{1-\xi_1} \frac{d\xi_2}{[y_0\xi_1 + \xi_2][p^2(\xi) - io]}, \tag{147}$$

with

$$\frac{p^2(\xi)}{4M_W^2} = \xi_2^2(1-\zeta) + \xi_1\xi_2(-1-\zeta+x_s+1/x_s) + \xi_1 + \xi_2\zeta + \frac{m_1^2}{M_W^2}(1-\xi_1-\xi_2)^2. \tag{148}$$

We perform the following change of variables:

$$\xi_1 = \frac{1}{1+t+u} \quad \text{and} \quad \xi_2 = \frac{t}{1+t+u}. \tag{149}$$

Accordingly, the area of integration changes from

$$\xi_1 > 0, \quad \xi_2 > 0, \quad \xi_1 + \xi_2 < 1, \tag{150}$$

to

$$0 < t < \infty, \quad 0 < u < \infty. \tag{151}$$

The Jacobian of the transformation is given by

$$\left| \frac{\partial(\xi_1 \xi_2)}{\partial(tu)} \right| = \frac{1}{[1 + u + t]^3}. \tag{152}$$

The final integral to be evaluated looks like

$$M_W^2 D_{0123} = -\frac{i}{16\pi^2 D_2} \int\limits_0^\infty \frac{du\, dt}{[y_0 + t][t^2 + t(x_s + 1/x_s) + 1 + u(1 + t\zeta) + \frac{m_1^2}{M_W^2} u^2]}. \tag{153}$$

The second expression in the denominator of the integrand is linear in u up to the small term $u^2\, m_1^2/M_W^2$, which is needed to regularize the collinear divergences of the integral. When performing partial fractioning of the integrand, this term should not be neglected; it has to be treated as a small parameter.

Performing first the integration over u and then the integration over t, we obtain the final result (62) for D_{0123}, expressed in terms of logarithms and dilogarithms.

A.3 The infrared-divergent four-point function

Next we present a few steps in the calculation of the Feynman-parameter integral belonging to D_{0134} (see Sect. 3.2.3). The first step involves the integration over momentum space, as represented by Eq. (68). The contour will be closed in the lower half of the complex k_0-plane, where only one pole is situated at $k_0 = \sqrt{\vec{k}^2 + \lambda^2 - io}$. We introduce cylindric variables in the $\vec{p}(\xi)$ direction:

$$I_{0134}(\xi) = -\frac{i}{8\pi^2} \int \frac{\rho\, d\rho\, dz}{\sqrt{\rho^2 + z^2 + \lambda^2}\, \left[-|E(\xi)| \sqrt{\rho^2 + z^2 + \lambda^2} - |\vec{p}(\xi)|\, z + A(\xi) + io \right]^3}. \tag{154}$$

The integration over ρ becomes trivial:

$$I_{0134}(\xi) = \frac{i}{16\pi^2 |E(\xi)|} \int\limits_{-\infty}^{\infty} \frac{dz}{\left[-|E(\xi)| \sqrt{z^2 + \lambda^2} - |\vec{p}(\xi)|\, z + A(\xi) + io \right]^2}. \tag{155}$$

The last integration simplifies if one uses the representation:

$$I_{0134}(\xi) = \frac{i}{16\pi^2 \lambda\, |E(\xi)|} \frac{\partial}{\partial |E(\xi)|} \left\{ \int\limits_{-\infty}^{\infty} \frac{dz}{\sqrt{z^2 + 1} \left[-|E(\xi)| \sqrt{z^2 + 1} - |\vec{p}(\xi)|\, z + A(\xi)/\lambda + io \right]} \right\}. \tag{156}$$

Introducing the standard variable transformation $t = \sqrt{z^2+1} - z$, the final integration can be performed, leading to the result given in Eq. (70).

The second stage of the calculation involves the integration over the Feynman parameters. We start with Eq. (70). This time we combine a change of variables, analogous to the one utilized in the previous appendix, with a rescaling :

$$\xi_3 = \frac{t}{1+u+t}, \quad \xi_2 = \frac{1}{1+u+t} \quad \text{followed by} \quad t \to \frac{M_W}{m_2} t, \quad u \to \frac{M_W}{m_1} u. \tag{157}$$

In this way D_{0134} takes the form

$$D_{0134} = -\frac{i}{4\pi^2} \frac{M_W^2}{m_1 m_2} \int_0^\infty du\, dt\, \frac{\partial}{\partial p'^2} \left\{ \frac{1}{\sqrt{A'^2 - \lambda^2 p'^2}} \ln\left(\frac{A' - \sqrt{A'^2 - \lambda^2 p'^2}}{A' + \sqrt{A'^2 - \lambda^2 p'^2}} \right) \right\}, \tag{158}$$

where the definitions of A' and p'^2 have now changed. Those quantities are rescaled versions of A and p^2. The rescaling is performed in such a way that p'^2 changes to

$$\frac{p'^2}{4M_W^2} = t^2 + u^2 - \frac{s_{12}}{m_1 m_2} tu + \frac{\zeta' M_W}{m_2} t + \frac{M_W}{m_1} u + 1. \tag{159}$$

In order to linearize this expression with respect to u, one has to introduce one more variable transformation

$$t = t' + c\, u, \quad \text{with} \quad c = \frac{m_1 m_2}{s_{12}}, \tag{160}$$

which leads to

$$\frac{p'^2}{4M_W^2} = t'^2 - \frac{s_{12}}{m_1 m_2} t' u + \frac{\zeta' M_W}{m_2} t' + \frac{M_W}{m_1} u + 1. \tag{161}$$

After changing the order of integration according to

$$\int_0^\infty du \int_0^\infty dt \to \int_0^\infty du \int_{-cu}^\infty dt' = \int_0^\infty dt' \int_0^\infty du + \int_{-\infty}^0 dt' \int_{-t'/c}^\infty du, \tag{162}$$

one can perform the rest of the Feynman-parameter integrations to obtain the final result (72) for D_{0134}.

B Why $\mathcal{R}$ vanishes

In this appendix it will be shown that the second term in Eq. (33), given by

$$\mathcal{R} = \int \frac{d^4k}{(2\pi)^4 N_0} \mathcal{P}ole \frac{\sum r_i (k \cdot v_i) + 2a\lambda^2}{N_1 N_2 N_3 N_4}, \tag{163}$$

is actually zero. In this integral the photon is not necessarily on-shell, because the residue is not taken in the photon pole. However, by power counting we can conclude that only soft photons

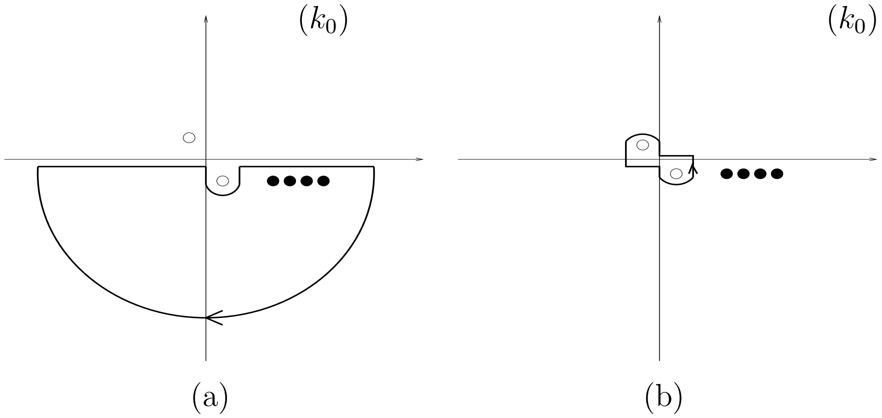

Figure 6: The pole structure of $\mathcal{R}$ in the soft-photon approximation (a) and the transformation of the integration contour in the complex k_0-plane (b). The solid circles indicate the particle poles, the open circles the photon poles.

give a noticeable contribution to the integral. All other contributions are formally of higher order in the expansion in powers of Γ_W/M_W. Therefore we use the soft-photon approximation to evaluate this integral. As a result, all particle poles are situated in the same half-plane of the complex k_0 variable, as is shown in Fig. 6(a).

Next one can deform the integration contour in the way depicted in Fig. 6(b). Note that the orientation of the contour is reversed. Figure 6 shows that the sum of the particle-pole residues is equal to the sum of the photon-pole residues with the opposite sign. This is a consequence of the soft-photon approximation and of the fact that all particle poles turned out to be in the same half-plane of the complex k_0 variable. The latter is the result of the transformation (28) introduced in Sect. 2.2.

Let us consider the following general integral

$$\mathcal{R}(p) = \int \frac{d^4k}{(2\pi)^4 N_0}\, \mathcal{P}ole\, \frac{p\cdot k}{N_1 N_2 N_3 N_4}, \tag{164}$$

where p^μ is an arbitrary vector. In the soft-photon approximation the denominators can be written as $N_0 = k^2 - \lambda^2 + io$ and $N_i = 2(p_i\cdot k) + p_i^2 - m_i^2 + io$. As mentioned in Sect. 2.2, the momenta p_i are time-like and have positive energy components, i.e. $E_i \geq |\vec{p}_i|$. For simplicity we take the photon to be massless, i.e. $\lambda^2 = 0$, but the arguments that follow do not depend on this. Deforming the integration contour as described above, and subsequently taking the residues in the photon poles, one can write

$$\mathcal{R}(p) = 2\pi i \int \frac{d^3k}{(2\pi)^4\, 2\omega}\, \frac{(p\cdot k)}{N_1N_2N_3N_4}\bigg|_{\omega=-|\vec{k}|+io} + 2\pi i \int \frac{d^3k}{(2\pi)^4\, 2\omega}\, \frac{(p\cdot k)}{N_1N_2N_3N_4}\bigg|_{\omega=|\vec{k}|-io}. \tag{165}$$

In spherical coordinates this takes the form

$$\begin{aligned}\mathcal{R}(p) &= i\pi \int_0^\infty \frac{d|\vec{k}|\, d^2\Omega_k}{(2\pi)^4}\, \frac{|\vec{k}|^2\,(E + f(\Omega_k)|\vec{p}|)}{\prod_{i=1}^4 \Big[-2|\vec{k}|\,(E_i + f_i(\Omega_k)|\vec{p}_i|) + p_i^2 - m_i^2 + io\Big]} \\ &+ i\pi \int_0^\infty \frac{d|\vec{k}|\, d^2\Omega_k}{(2\pi)^4}\, \frac{|\vec{k}|^2\,(E - f(\Omega_k)|\vec{p}|)}{\prod_{i=1}^4 \Big[2|\vec{k}|\,(E_i - f_i(\Omega_k)|\vec{p}_i|) + p_i^2 - m_i^2 + io\Big]}.\end{aligned} \tag{166}$$

In the second term one can make a change of variables according to $|\vec{k}| \to -|\vec{k}|$ and $\vec{n}_k \to -\vec{n}_k$, to obtain

$$\mathcal{R}(p) = i\pi \int_{-\infty}^{\infty} \frac{d|\vec{k}|\, d^2\Omega_k}{(2\pi)^4}\, \frac{|\vec{k}|^2\,(E + f(\Omega_k)|\vec{p}|)}{\prod_{i=1}^4 \Big[-2|\vec{k}|\,(E_i + f_i(\Omega_k)|\vec{p}_i|) + p_i^2 - m_i^2 + io\Big]}. \tag{167}$$

This integral is ultraviolet-finite and all poles are situated in the same half-plane of the complex variable $|\vec{k}|$, since $E_i \geq |\vec{p}_i|$ and $|f_i(\Omega_k)| \leq 1$. By closing the contour in the opposite half-plane, one finds $\mathcal{R}(p) = 0$. From this it trivially follows that $\mathcal{R} = 0$.

C Special functions and integrals in the DMI method

C.1 The functions F_1 and F_2

In this appendix we present the functions F_1 and F_2, which are used in the calculations in Sect. 4. The function F_1 is defined as

$$F_1(a;\beta|x_i) = \int_{-1}^{1} \frac{dx}{x-a}\, \ln(1+\beta x)\, \Big[\theta(x-x_i) - \theta(x_i - x)\Big]. \tag{168}$$

Here a is a complex number with a non-zero imaginary part, and β and x_i are real numbers with absolute value smaller than 1. The analytical expression for this function is given by

$$\begin{aligned}F_1(a;\beta|x_i) &= -2\,\mathrm{Li}_2\Big(\frac{1+x_i\beta}{1+a\beta}\Big) + \mathrm{Li}_2\Big(\frac{1-\beta}{1+a\beta}\Big) + \mathrm{Li}_2\Big(\frac{1+\beta}{1+a\beta}\Big) + \ln\Big(\frac{\beta(1+a)}{1+a\beta}\Big)\ln(1-\beta) \\ &+ \ln\Big(\frac{\beta(a-1)}{1+a\beta}\Big)\ln(1+\beta) - 2\ln\Big(\frac{\beta(a-x_i)}{1+a\beta}\Big)\ln(1+x_i\beta).\end{aligned} \tag{169}$$

In addition we need this function in the special case $a = x_i$, without non-zero imaginary part. There, the integral $F_1(x_i;\beta|x_i)$ is logarithmically divergent. This is a collinear divergence and should be regularized by keeping the small non-zero fermion masses. The answer in this case is

$$F_1(x_i;\beta|x_i) = \ln(1+x_i\beta)\ln\Bigl(\frac{4E_i^2}{m_i^2}\Bigr) - \mathrm{Li}_2\Bigl(\beta\frac{1+x_i}{1+x_i\beta}\Bigr) - \mathrm{Li}_2\Bigl(\beta\frac{x_i-1}{1+x_i\beta}\Bigr). \tag{170}$$

The other function, F_2, is defined as

$$F_2(a|x_i) = \int\limits_{-1}^{1} \frac{dx}{x-a}\,\Bigl[\theta(x-x_i) - \theta(x_i-x)\Bigr]. \tag{171}$$

For a and x_i the same restrictions as indicated for the function F_1 apply. The corresponding analytical expressions are

$$F_2(a|x_i) = -2\ln(x_i-a) + \ln(-1-a) + \ln(1-a), \tag{172}$$

and

$$F_2(x_i|x_i) = \ln\Bigl(\frac{4E_i^2}{m_i^2}\Bigr). \tag{173}$$

C.2 The azimuthal principal-value integral

In this appendix we present the result for the azimuthal principal-value integral, used in Sect. 4:

$$I_\phi = \mathcal{P}\left(\int\limits_0^{2\pi}\frac{d\phi}{2\pi}\,\frac{1}{A-B\cos\phi}\right), \tag{174}$$

with

$$A = (v_1 - v_2\cos\theta_{12})\,\cos\theta \quad \text{and} \quad B = v_2\sin\theta_{12}\sin\theta. \tag{175}$$

The principal-value integration yields

$$I_\phi = \begin{cases} +\frac{1}{\sqrt{A^2-B^2}} & \text{for} \quad A/B \in (+1,+\infty) \quad \text{or equivalently} \quad \cos\theta \in (+x_+,+1) \\ -\frac{1}{\sqrt{A^2-B^2}} & \text{for} \quad A/B \in (-\infty,-1) \quad \text{or equivalently} \quad \cos\theta \in (-1,-x_+) \end{cases}, \tag{176}$$

where

$$x_+ = \sqrt{\frac{v_2^2(1-x_{12}^2)}{v_1^2+v_2^2-2v_1v_2x_{12}}} \quad \text{and} \quad \sqrt{A^2-B^2} = |\vec{v}_1-\vec{v}_2|\,\sqrt{x^2-x_+^2}. \tag{177}$$

In non-collinear situations one can take $v_{1,2}\to 1$, resulting in $x_+ = \sqrt{(1+x_{12})/2}\,$.

C.3 The functions $\mathcal{F}_1$, $\mathcal{F}_2$ and $\mathcal{K}$

In this appendix we present the functions $\mathcal{F}_1$, $\mathcal{F}_2$, and $\mathcal{K}$, used in Sect. 4 for the infrared-divergent four- and five-point functions.

The function $\mathcal{F}_1$ is defined as

$$\mathcal{F}_1(x_+;v) = \int\limits_{x_+}^{1} \frac{dx}{\sqrt{x^2 - x_+^2}} \frac{1}{1-vx} \ln\Big(\frac{1-vx}{1+vx}\Big). \tag{178}$$

Here, x_+ is real with $0 \le x_+ < 1$, and the quantity v is real and close to unity. For $v \to 1$ the answer for this integral is given by

$$\mathcal{F}_1(x_+;v) = \frac{1}{\sqrt{1-x_+^2}} \Big[-\frac{1}{2}\ln^2\Big(\frac{1-v}{2}\Big) - \frac{\pi^2}{6} + \frac{1}{2}\ln^2(1-x_+^2) - \ln(x_+)\,\ln(1-x_+^2)\Big]. \tag{179}$$

The function $\mathcal{F}_2$ is defined as

$$\mathcal{F}_2(x_+) = \int\limits_{x_+}^{1} \frac{dx}{\sqrt{x^2 - x_+^2}} \frac{1}{1+x} \ln\Big(\frac{1-x}{1+x}\Big), \tag{180}$$

which amounts to

$$\mathcal{F}_2(x_+) = \frac{1}{\sqrt{1-x_+^2}} \Big[\mathrm{Li}_2(x_+^2) - \frac{\pi^2}{6} + \ln(x_+)\,\ln(1-x_+^2)\Big]. \tag{181}$$

In our explicit formulae, the functions $\mathcal{F}_1$ and $\mathcal{F}_2$ always enter as a sum. This sum can be represented in a compact form:

$$\mathcal{F}_1(x_+;v) + \mathcal{F}_2(x_+) = \frac{1}{\sqrt{1-x_+^2}} \Big[-\frac{1}{2}\ln^2\Big(\frac{1-v}{2}\Big) - \mathrm{Li}_2\Big(\frac{x_+^2}{x_+^2-1}\Big) - \frac{\pi^2}{3}\Big]. \tag{182}$$

The function $\mathcal{K}$ is defined as

$$\mathcal{K}(A;B|x_0;\mu^2) = \int\limits_{-1}^{1} \frac{dx}{(x+A)\sqrt{(x-x_0)^2+\mu^2}} \ln(B-x), \tag{183}$$

A being a complex number with a non-zero imaginary part, and B being real and larger than 1. The quantities x_0 and μ are real, with $|x_0| < 1$ and $\mu^2 \ll 1$. The resulting analytical expression is somewhat more complicated:

$$\begin{aligned}\mathcal{K}(A;B|x_0;\mu^2) = \frac{-1}{A+x_0}\Big\{ &\mathcal{L}\mathrm{i}_2\Big(1;\frac{A+1}{A+x_0}\Big) - \mathcal{L}\mathrm{i}_2\Big(1;\frac{A+x_0}{A-1}\Big) - \mathcal{L}\mathrm{i}_2\Big(\frac{B-x_0}{B-1};\frac{A+1}{A+x_0}\Big) \\ &+ \mathcal{L}\mathrm{i}_2\Big(\frac{B+1}{B-x_0};\frac{A+x_0}{A-1}\Big) - \frac{1}{2}\ln^2\Big(\frac{B-x_0}{B-1}\Big) + \ln(B-1)\,\ln\Big(\frac{A+1}{A+x_0}\Big) \\ &+ \ln(B-x_0)\ln\Big(\frac{\mu^2}{4(1-x_0^2)}\frac{A-1}{A+x_0}\Big)\Big\}. \end{aligned} \tag{184}$$

References

[1] W. Beenakker and A. Denner, *Int. J. Mod. Phys.* **A9** (1994) 4837;
W. Beenakker et al., *hep–ph/*9602351, in *Physics at LEP2*, eds. G. Altarelli, T. Sjöstrand and F. Zwirner (CERN 96-01, Geneva, 1996), Vol. 1, p. 79.

[2] E.N. Argyres et al., *Phys. Lett.* **B358** (1995) 339;
W. Beenakker et al., *hep–ph/*9612260.

[3] A. Aeppli, G.J. van Oldenborgh and D. Wyler, *Nucl. Phys.* **B428** (1994) 126.

[4] W. Beenakker, A.P. Chapovsky and F.A. Berends, *hep–ph/*9706339.

[5] V.S. Fadin, V.A. Khoze and A.D. Martin, *Phys. Lett.* **B320** (1994) 141; *Phys. Rev.* **D49** (1994) 2247;
K. Melnikov and O. Yakovlev, *Phys. Lett.* **B324** (1994) 217.

[6] V.S. Fadin and V.A. Khoze, *Yad. Fiz.* **48** (1988) 487; *Sov. J. Nucl. Phys.* **48** (1988) 309;
V.S. Fadin, V.A. Khoze and A.D. Martin, *Phys. Lett.* **B311** (1993) 311.

[7] D. Bardin, W. Beenakker and A. Denner, *Phys. Lett.* **B317** (1993) 213.

[8] V.S. Fadin et al., *Phys. Rev.* **D52** (1995) 1377.

[9] K. Melnikov and O. Yakovlev, *Nucl. Phys.* **B471** (1996) 90.

[10] G. Gounaris et al., *hep–ph/*9601233, in *Physics at LEP2*, eds. G. Altarelli, T. Sjöstrand and F. Zwirner (CERN 96-01, Geneva, 1996), Vol. 1, p. 525.

[11] W.L. van Neerven and J.A.M. Vermaseren, *Phys. Lett.* **B137** (1984) 241.

[12] A. Denner, U. Nierste and R. Scharf, *Nucl. Phys.* **B367** (1991) 637.

[13] G.J. van Oldenborgh and J.A.M. Vermaseren, *Z. Phys.* **C46** (1990) 425;
G. 't Hooft and M. Veltman, *Nucl. Phys.* **B153** (1979) 365.